

## **Vertical mixing and restratification in the Bay of Bothnia during cooling**

by Anders Omstedt and Jörgen Sahlberg

Norrköping 1982



**SMHI**

Box 923  
S-Norrköping

# **Vertical mixing and restratification in the Bay of Bothnia during cooling**

by Anders Omstedt and Jörgen Sahlberg



## FOREWORD

The Winter Navigation Research Board presents its report no. 35. The report describes an advanced mathematical model by which the cooling rate and the changes of vertical temperature profiles in enclosed basins can be calculated using meteorological parameters. The model has been adjusted to the Bay of Bothnia and tested against actual vertical temperature measurements during an autumn cooling period. The results presented are very promising.

The study is a part of a thermodynamic ice project aiming at the forecasting of water cooling, ice formation, growth and decay.

The Winter Navigation Research Board expresses its thanks to the authors and those who have assisted them in their work.

Norrköping and Helsinki, March 1982

Kaj Janérus

Jan-Erik Jansson

## ABSTRACT

Autumn cooling in the Bay of Bothnia provides an opportunity for studying wind mixing, convection and restratification below the temperature for maximum density. Vertical temperature profiles for a 52 day period are analysed for the case of cooling of brackish sea water around the temperature of maximum density. A mathematical model, which is based on the conservation equations for momentum, heat and salt in their one-dimensional form and with an equation of state which is linear with respect to salinity but quadratic with respect to temperature, is presented. Turbulent exchange coefficients are calculated with a kinetic energy-dissipation model of turbulence.

Due to the fact that both salinity and temperature effect stratification and that buoyancy flux changes sign at the temperature for maximum density several processes influence the cooling rate. The mathematical model describes these and the general development of the temperature profiles in a most satisfactory way.

## SAMMANFATTNING

Höstavkylningen av Bottenvikens vattenmassa ger möjlighet till studier av vindblandning och konvektion för temperaturer runt temperaturen för maximal täthet. Under en 52-dagars period 1979 mättes vattentemperaturen på 22 olika djup. Dessa data har dygnsmedelvärdesbildats och analyserats. En matematisk modell presenteras här. Den är baserad på en-dimensionella konservationsekvationer för momentum, värme och salt tillsammans med en tillståndsekvation som är linjärt beroende på salthalt och kvadratisk på temperatur. De turbulenta utbyteskoefficienterna beräknas med en turbulensmodell (k- $\epsilon$  modell).

Den matematiska modellen beskriver förändringarna hos de mätta temperaturprofilerna på ett tillfredsställande sätt.

## TABLE OF CONTENT

	Page
1. INTRODUCTION	1
2. GENERAL DESCRIPTION	4
3. MODEL EQUATIONS	5
3.1 <u>Basic assumptions</u>	5
3.2 <u>Mean flow equations</u>	6
3.3 <u>Equation of state</u>	7
3.4 <u>Turbulence equations</u>	10
3.5 <u>Processes at the air-sea interface</u>	12
4. MODEL ILLUSTRATIONS	15
4.1 <u>Introduction</u>	15
4.2 <u>Cooling of brackish sea water</u>	16
4.3 <u>Different eddy viscosity assumptions</u>	18
5. MODEL APPLICATION TO THE BAY OF BOTHNIA	21
5.1 <u>Water temperature data</u>	21
5.2 <u>Meteorological data</u>	23
5.3 <u>Comparison between calculated and observed temperatures</u>	24
6. SUMMARY AND CONCLUSIONS	30
Acknowledgements	32
Literature references	33
Nomenclature	38



## 1. INTRODUCTION

Under the joint Swedish-Finnish winter navigation research programme the Swedish Meteorological and Hydrological Institute (SMHI) is participating with a programme in which the interaction between atmosphere, ice and sea is studied. One project within this programme treats cooling and freezing in the Bay and Sea of Bothnia. The time of the year when ice starts to form is very variable due to differences in meteorological forcing from year to year, figure 1. It is therefore of great interest for shipping and icebreaking service to get information about changes in sea surface temperatures during autumn cooling as a first information on how soon ice will form.

A simple thermodynamic model for the large scale cooling in the Bay of Bothnia is now used at SMHI, Sahlberg and Törnevik (1980). The model, however, just treats the whole Bay of Bothnia as one layer and therefore neglect the importance of varying temperatures with depth, which are of particular importance before ice formation. The purpose of this paper is to present a model which could calculate the vertical variations in the temperatures during cooling of brackish sea water, that means water with less salinity than  $24.7^{\circ}/\text{oo}$ , down to the freezing point.

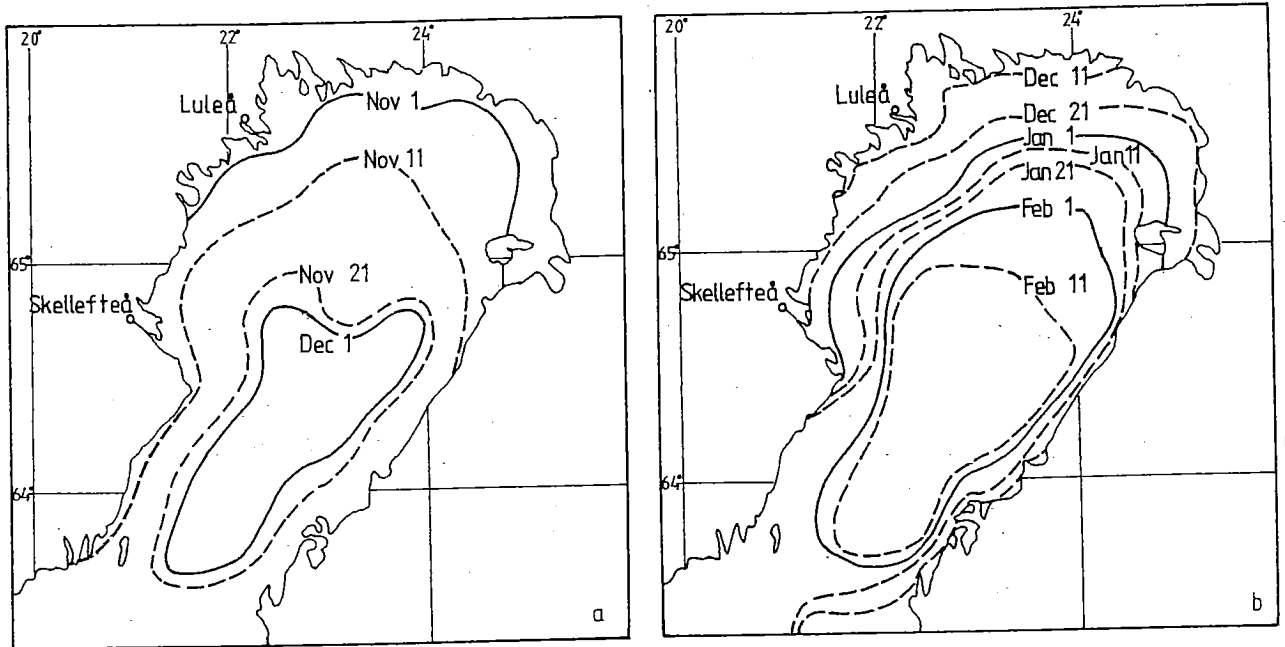


Figure 1 The charts show the dates for the first (a) and latest day (b) of ice formation in the Bay of Bothnia, SMHI and FIMR (1982).

In water with a salinity less than  $24.7^{\circ}/\infty$ , vertical convection continues until the temperature for maximum density ( $T_{\rho m}$ ) is reached, figure 2. Further cooling causes a change in sign of buoyancy flux and creates a restratification which increases the cooling rate.

Many attempts have been made to predict changes in the sea surface layer due to different meteorological conditions. One dimensional models have often been used as temperature and salinity often varies more along vertical axis than horizontal. A discussion of different kinds of one dimensional models for the upper ocean is made by Niiler and Kraus (1977).

The modelling of brackish sea water during autumn and winter cooling has received little attention in the literature, but the temperatures for maximum density and freezing have been considered frequently and these equations are well documented.

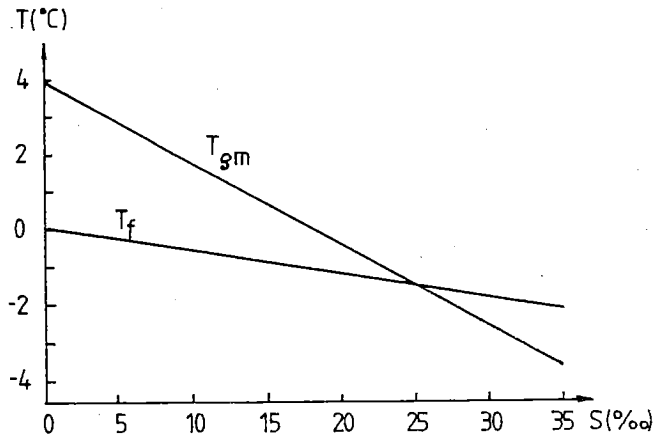


Figure 2 The temperature for maximum density ( $T_{\rho m}$ ) and the temperature for freezing point ( $T_f$ ).

Several other studies provide useful information for the problem addressed. To be mentioned are the studies of salinity effects in the ocean mixed layer by Miller (1976) and the numerical simulation of thermohaline convection by Delnore (1980). Miller (1976) showed that the most significant effects produced by the inclusion of salinity are the reduction of the deepening rate and the corresponding change in the heating characteristics of the mixed layer.

Delnore (1980) also pointed out the necessity of including gradient information for both temperature and salinity in modelling the diurnal heating cycle of the ocean.

It is also noted that the non linearity and pressure dependence in the equation of state for cooling of deep lakes have been discussed by Farmer and Carmack (1981).

One main problem in modelling the upper layer of the sea is the formulation of the turbulence processes. A wide spectrum of turbu-

lence models is now available. At present a two-equation model, with one equation for the turbulent kinetic energy and the other for the dissipation of turbulent kinetic energy, is most widely tested one for hydraulic flow problems, Rodi (1980).

This kind of turbulence model has also been used for modelling the seasonal thermocline in lakes, in studying the structure of the turbulent Ekman layer, Svensson (1978, 1979) and calculating the turbulent boundary layer under drifting sea ice, Svensson (1981).

The present study extends this turbulent model to the Bay of Bothnia, where the stratification depends mainly on temperature and salinity. The purpose is to analyse measured temperatures for a 52 days cooling period from October 23 to December 13 1979 and to develop a model for autumn cooling.

## 2. GENERAL DESCRIPTION

The Bay of Bothnia is the northern extension of the Baltic. Climatologically it is situated in the northern part of the westerlies and therefore the weather is influenced by the meandering polar front and the disturbances on it which during late autumn could cause strong winds. During late autumn and winter the low pressure systems normally pass south of the area and cold air masses cover the whole bay.

The Bay of Bothnia has a typical estuary circulation with lighter fresh water from rivers mixed with the under-lying saltier water. The water exchange with the Sea of Bothnia goes through the Northern Quark. The amount of saltier water going from the Sea of Bothnia to the Bay of Bothnia is about  $400 \text{ km}^3 \text{ year}^{-1}$  and the amount of less saltier water leaving the Bay of Bothnia is about  $500 \text{ km}^3 \text{ year}^{-1}$ . In late autumn and in winter the water is two layered. The depth of the upper layer varies between 30-50 m and has a salinity of  $3.0-3.5\text{‰}$ , while the bottom layer salinity is in the range of  $4.0-4.5\text{‰}$ . Tidal effects are negligible, but water level variations mainly due to wind and air pressure exist with amplitudes in the order of one meter. Maximum water depth is 126 m, while the mean depth is 41 m and the Northern Quark sill depth 20 m. A typical residence time for the water in the Bay of Bothnia is about 3 years which is a rather slow process compared

with autumn cooling. It might thus be expected that cooling in the main basin is mostly influenced by the heat exchange through the air-water interface.

During autumn the cooling causes horizontal temperature gradients due to water depth variations close to the coast. In the main basin however the horizontal temperature gradients are less pronounced.

The internal hydrographic response in a system like the Bay of Bothnia is mainly baroclinic in a narrow coastal region, while the response in the main basin is essentially barotropic, Walin (1972). This means that in the main basin, temperature and salinity surfaces are horizontal and one dimensional approach could be possible.

For the cooling rate the heat loss at the air-sea interface and the mixing depth are of most importance. The mixing depth depends mainly on wind mixing, convection and restratification when cooling has passed the temperature of maximum density. These processes can be well described by one dimensional boundary layer theory.

### 3. MODEL EQUATIONS

#### 3.1 Basic assumptions

The study will restrict attention to horizontally homogeneous flows which means that terms containing gradients in the horizontal plane are neglected. It is further assumed that there is no mean vertical velocity. Short wave radiation is known to penetrate the water body following an exponential decay. During the period considered the solar radiation is however of minor importance and will therefore be treated as a surface flux of heat. Gravitational effects are assumed to follow the Boussinesq approximation. A schematic representation of the mathematical model as applied to the Bay of Bothnia is given in figure 3. The variation of horizontal area versus depth is in accordance with the Bay of Bothnia. This is of fundamental importance when modelling changes in the total heat content, Svensson (1978).

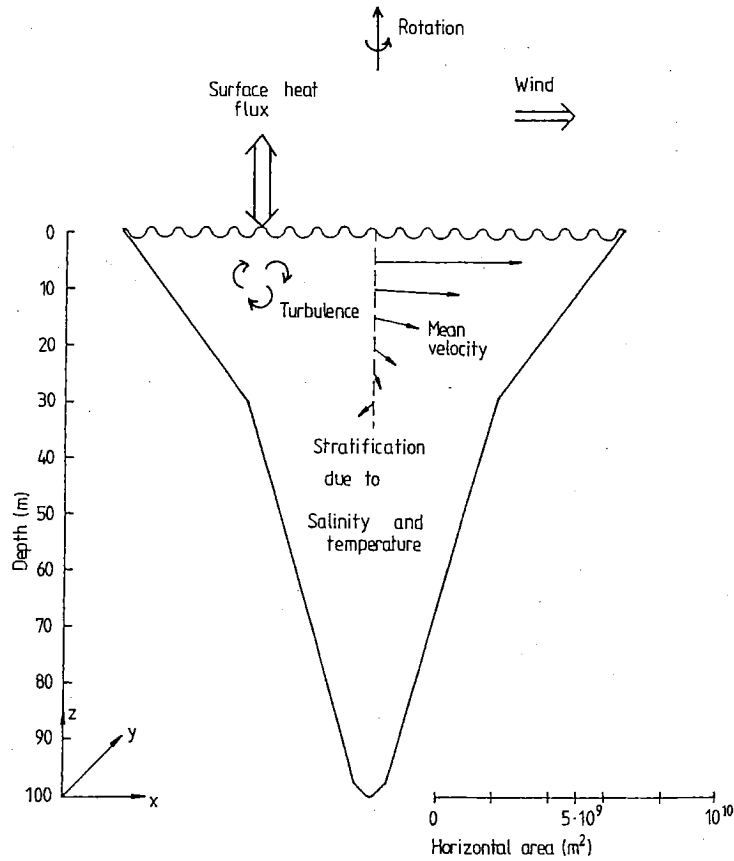


Figure 3 Schematic representation of the one dimensional model for the Bay of Bothnia.

### 3.2 Mean flow equations

Primarily the temperature distribution is of interest but a few more variables are needed to describe the problem. Salinity is one of them and another is the velocity distribution which, needs to be considered since turbulence is to a large extent produced by shear. With the assumptions made the equations for the variables read:

$$\frac{\partial T}{\partial t} = \frac{\partial}{\partial z} (-\overline{w\theta} + \kappa \frac{\partial T}{\partial z}), \quad (1)$$

$$\frac{\partial S}{\partial t} = \frac{\partial}{\partial z} (-\overline{ws} + \kappa_s \frac{\partial S}{\partial z}), \quad (2)$$

$$\frac{\partial U}{\partial t} = \frac{\partial}{\partial z} (-\overline{wu} + \nu \frac{\partial U}{\partial z}) + fV, \quad (3)$$

$$\frac{\partial V}{\partial t} = \frac{\partial}{\partial z} (-\overline{wv} + \nu \frac{\partial V}{\partial z}) - fU, \quad (4)$$

where  $Z$  is the vertical space coordinate, positive upwards,  $t$  time coordinate,  $f$  Coriolis parameter,  $U$  and  $V$  mean velocities in horizontal directions,  $T$  mean temperature,  $S$  mean salinity,  $\nu$  molecular kinematic viscosity,  $\kappa$  molecular thermal diffusivity and  $\kappa_s$  molecular diffusivity for salt. The correlation terms  $\overline{wu}$ ,  $\overline{wv}$ ,  $\overline{w\theta}$  and  $\overline{ws}$  represent Reynold stresses and turbulent transport of heat and salt respectively.

Boundary conditions for the mean flow equations at the surface are specified according to:

$$\left(-\overline{wu} + \nu \frac{\partial U}{\partial Z}\right) = \frac{\tau_x(t)}{\rho_0}, \quad (5)$$

$$\left(-\overline{wv} + \nu \frac{\partial V}{\partial Z}\right) = \frac{\tau_y(t)}{\rho_0}, \quad (6)$$

$$\left(-\overline{ws} + \kappa_s \frac{\partial S}{\partial Z}\right) = 0, \quad (7)$$

$$\left(-\overline{w\theta} + \kappa \frac{\partial T}{\partial Z}\right) = \frac{Q(t)}{\rho_0 C_p}, \quad (8)$$

where  $\rho_0$  is the water density,  $\tau_x(t)$  and  $\tau_y(t)$  wind stresses,  $C_p$  specific heat of water and  $Q(t)$  net heat flux.  $Q(t)$  is of course a sum of several processes as sensible heat flux, latent heat flux and radiation fluxes. They will be discussed further in chapter 3.5. The zero flux condition for salinity is an approximation since advection from rivers, precipitation and evaporation in effect generate a non zero flux. At the lower boundary a zero flux condition is used for all variables, the reason being that this boundary is positioned well below the depth of surface influence and the deep water flow due to estuary circulation is neglected.

The mean flow equations however do not form a closed system due to the turbulence correlation terms. An equation for the turbulence is therefore needed, but first the equation of state has to be studied.

### 3.3 Equation of state

The equation of state for sea water describes the relation between

salinity, temperature, pressure and density. From very accurate measurements in the Baltic in the beginning of this century, Knudsen et al (1901) constructed hydrographical tables for density. These tables are still in use and later measurements have shown that they are in good agreement when salinity is higher than  $15\text{‰}$ , Kremling (1972). At lower salinities the comparison differs due to input of dissolved river salts into the Baltic and an other chlorinity-salinity relation has to be used when determining the density for low salinity water, Miller and Kremling (1976). Pressure effects both the density and the temperature for maximum density. This has been treated by Farmer and Carmack (1981) in a study of cooling in a deep fresh water lake. As a lake cools through the temperature for maximum density, the thermal expansion coefficient becomes critically dependent on pressure and a phase where stratification is mainly pressure sensitive is reached. The importance of the pressure effects increases rapidly with depth. In the Bay of Bothnia salinity gradient however inhibits convection to deeper layer why pressure effects have been neglected.

As the relationship between salinity, temperature and density is nonlinear and rather complicated a simplified equation of state is used. This equation should reproduce the almost quadratic relation between temperature and density around the point of maximum density and also the linear dependence on salinity, figure 4.

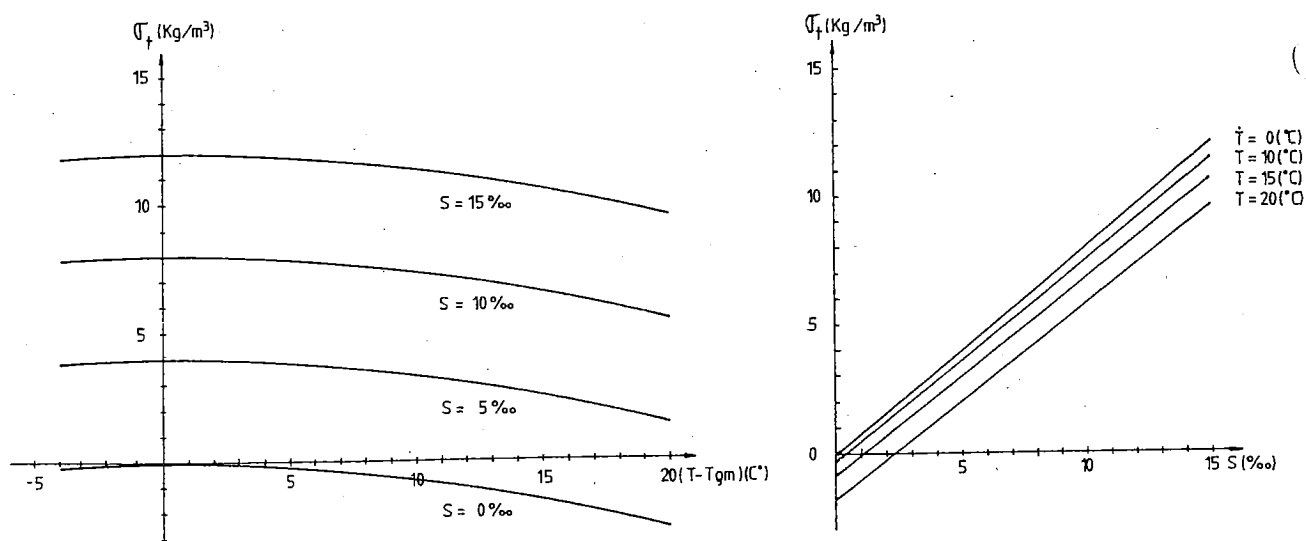


Figure 4 The density of sea water as a function of temperature and salinity.

The equation of state used in this study reads:

$$\rho = \rho_0 (1 - \alpha(T - T_{\rho m})^2 + \beta s) \quad (9)$$

where  $\alpha$  and  $\beta$  are constants and  $T_{\rho m}$  is the temperature of maximum density. The constants  $\alpha$  and  $\beta$  are chosen with respect to the temperature and salinity interval under consideration. In this study they are set to  $5.57 \cdot 10^{-6}$  and  $8.13 \cdot 10^{-4}$  respectively. The temperature of maximum density,  $T_{\rho m}$ , is strictly a function of salinity and pressure, Caldwell (1978). In this study  $T_{\rho m}$  is however set to a constant value of  $3.2^\circ\text{C}$  which is within  $\pm 0.1^\circ\text{C}$  accuracy for the mixed layer under consideration. As density variations are small a more useful density unit is Sigma-t ( $\sigma_t$ ) defined as

$$\sigma_t = \rho - 1000.$$

in SI-units.

A comparison between densities calculated from equation (9) and from Knudsen et al (1901) modified with a chlorinity-salinity relation according to Miller and Kremling (1976), is given in figure 5. The accuracy of equation (9) within the studied interval is  $\pm 0.03$  ( $\text{kg/m}^3$ ).

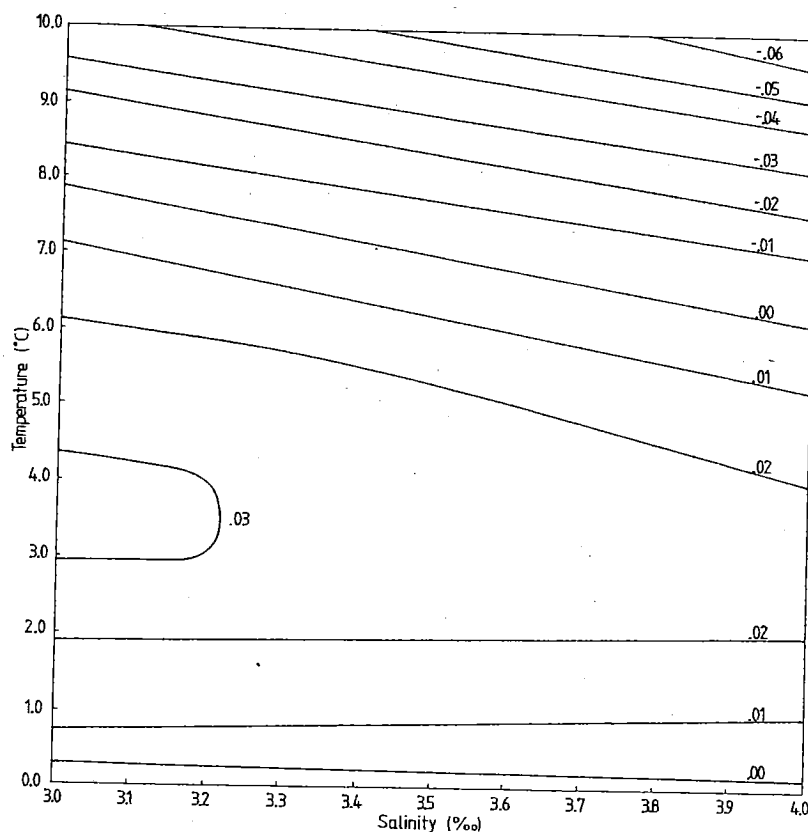


Figure 5 Error diagram in  $\sigma_t$ -units for sea water density according to Knudsen et al (1901) modified with a chlorinity-salinity relation according to Miller and Kremling (1976) and according to eq. (9).

The relative importance of the salinity stratification grows when the temperature for maximum density is reached and even very small changes in salinity can cause the density structure to look quite different. The relative importance between the salinity and temperature on density becomes:

$$\frac{\partial \rho}{\partial T} / \frac{\partial \rho}{\partial s} = 2 \frac{\alpha (T - T_{\rho m})}{\beta}$$

which, with coefficients according to this study, means that wiggles in temperature of 1°C around the temperature for maximum density could be stabilized by salinity variations of about 0.01‰/α. Small salinity variations in the upper sea surface layer are therefore of most importance for the density structure.

### 3.4 Turbulence equations

A fundamental process in mixed layer dynamics is the conversions of energy. Turbulent kinetic energy can be converted into potential energy. A budget equation for  $k$ , the turbulent kinetic energy, is needed. With the introduction of a kinematic eddy viscosity,  $\nu_T$ , a modelled form of the  $k$ -equation, see Launder and Spalding (1972) for details, reads:

$$\frac{\partial k}{\partial t} = \frac{\partial}{\partial z} \left( \frac{\nu_T}{\sigma_k} \frac{\partial k}{\partial z} \right) + \nu_T \left( \left( \frac{\partial U}{\partial z} \right)^2 + \left( \frac{\partial V}{\partial z} \right)^2 \right) + \frac{g}{\rho} \nu_T \frac{\partial \rho}{\partial z} - \epsilon, \quad (10)$$

where  $\sigma_k$  is a Prandtl/Schmidt number,  $g$  gravitational acceleration and  $\epsilon$  dissipation rate of  $k$ . Another advantage of solving an equation for  $k$  is that a velocity scale,  $k^{1/2}$ , is available for the determination of  $\nu_T$ . From physical reasoning and dimensional analysis it is expected that  $\nu_T$  is the product of a velocity scale and a length scale. Given the velocity scale a length scale is thus needed. If once again dimensional analysis is employed it can be shown that a length scale,  $l$ , can be obtained from  $k$  and  $\epsilon$  as:

$$l \sim k^{3/2} / \epsilon \quad (11)$$

Recalling that the velocity scale is  $k^{1/2}$ , the Prandtl/Kolmogorov relation for  $\nu_T$  is obtained:

$$v_T = C_\mu k^2 / \epsilon, \quad (12)$$

where  $C_\mu$  is an empirical constant. It remains to formulate an equation for  $\epsilon$  if  $v_T$  is to be calculated according to (12).

This equation is the weak point of most turbulence models present up to the date and some scientists argue that a prescribed length scale is as good as any dynamical equation presented. The success met by the  $\epsilon$ -equation in predicting a wide range of shear flows, see Rodi (1980) and Singhal and Spalding (1981), does indicate a certain degree of generality and the form of the  $\epsilon$ -equation given by these scientists is therefore employed:

$$\frac{\partial \epsilon}{\partial t} = \frac{\partial}{\partial z} \left( \frac{v_T}{\sigma_\epsilon} \frac{\partial \epsilon}{\partial z} \right) + C_{1\epsilon} v_T \frac{\epsilon}{k} \left( \left( \frac{\partial U}{\partial z} \right)^2 + \left( \frac{\partial V}{\partial z} \right)^2 \right) + C_{3\epsilon} \frac{g}{\epsilon \rho} \frac{v_T}{k} \frac{\partial \rho}{\partial z} - C_{2\epsilon} \frac{\epsilon^2}{k} \quad (13)$$

Having introduced the eddy-viscosity concept it is now possible to relate the turbulence correlations in the mean flow equations to their appropriate gradients through the following expressions:

$$\overline{-wu} = v_T \frac{\partial U}{\partial z}, \quad (14)$$

$$\overline{-wv} = v_T \frac{\partial V}{\partial z}, \quad (15)$$

$$\overline{-w\theta} = \frac{v_T}{\sigma_T} \frac{\partial T}{\partial z}, \quad (16)$$

$$\overline{-ws} = \frac{v_T}{\sigma_s} \frac{\partial S}{\partial z}, \quad (17)$$

where  $\sigma_T$  and  $\sigma_s$  are turbulent Prandtl/Schmidt numbers for temperature and salinity respectively. At present  $\sigma_T$  and  $\sigma_s$  are assumed to be constant, and equal to one, even if a dependence on stratification is known to exist.

The empirical constants appearing in the turbulence model are treated as being universal. For complex flows, i.e. recirculating, curved, etc, this universality may be questioned but for boundary flows the standard values, used in the present study and shown in Table 1, may be used with confidence.

Equations (1), (2), (3), (4), (9), (10), (12), (13), (14), (15), (16) and (17) form a closed system and thus constitute the formu-

lation of the mathematical model. This set of equations, in their finite difference form, were integrated forward in time with a time step of one hour, using an implicit scheme and a standard tridiagonal matrix algorithm. A complete derivation of the finite difference equations could be found in a paper by Svensson (1978). In chapter 4.3 different eddy viscosity assumptions and their consequence for cooling are discussed.

$C_{\mu}$	$C_{1\epsilon}$	$C_{2\epsilon}$	$C_{3\epsilon}$	$\sigma_k$	$\sigma_{\epsilon}$
0.09	1.44	1.92	0.8	1.0	1.3

Table 1 Constants in turbulence model

### 3.5 Processes at the air-sea interface

The processes at the air-sea interface should in general be treated as a three dimensional boundary layer problem, which means that both horizontal and vertical variations in the atmosphere should be considered. From atmospherical boundary layer experiments, bulk formulas have been determined which parameterize the heat and momentum exchange at the air-sea interface from a fixed level above the sea surface. With these bulk formulas the boundary layer is reduced to two dimensions and only horizontal variations in the atmosphere had to be considered.

In this work the cooling of the whole Bay of Bothnia is studied in a one dimensional sense. The horizontal variations in the atmosphere is therefore just treated by taking the input data for the bulk formulas as areal mean values over the whole basin. This is discussed in chapter 5.2.

The surface heat budget equation is

$$Q = Q_S + Q_L + Q_C + Q_E \quad (18)$$

where  $Q_S$  is the net short wave radiation,  $Q_L$  net long wave radiation,  $Q_C$  sensible heat flux and  $Q_E$  latent heat flux. During late autumn and in winter time the net short wave radiation ( $Q_S$ ) is of

minor importance. For a complete description  $Q_S$  is here taken into account and it becomes, see also Bodin (1979)

$$Q_S = (1-\alpha') T_u Q_o \cos Z' (T_R - A_w) \prod_{i=1}^3 (1 - N_i (1 - T_i)) \quad (19)$$

where  $\alpha'$  is the sea surface albedo,  $T_u$  the air turbidity,  $Q_o$  solar constant ( $1395 \text{ Wm}^{-2}$ ),  $Z'$  zenith angle,  $T_R$  transmission function,  $A_w$  absorption function,  $N_i$  amount of clouds of category  $i = 1, 2, 3$ ,  $T_i$  cloud function. The surface albedo is chosen as a function of the zenith angle according to Thompson (1979). Due to lack of turbidity data  $T_u$  is constant and equal to 1. The transmission function is

$$T_R = 1.041 - 0.16 (\text{Sec} Z')^{0.5}$$

given by Kondratyev (1969). The absorption function is

$$A_w = 0.077 (U \text{Sec} Z')^{0.3}$$

where  $U$  is the amount of precipitable water vapour content in the atmosphere in cm, Mc Donald (1960).

Low, middle or high clouds effect the short wave radiation differently. According to Pandolfo et al (1971) the cloud function is

$$T_i = a_i b_i \text{Sec} Z'$$

As the extracted weather data in this study only include one cloud coverage parameter, the constants  $a_i$  and  $b_i$  are chosen according to the middle high transmission function with the values of 0.45 and 0.01 respectively.

The net long wave radiation ( $Q_L$ ) consists of two parts, one going from the sea surface to the atmosphere ( $Q_{L\uparrow}$ ) and one going from the atmosphere to the sea surface ( $Q_{L\downarrow}$ ). The outgoing long wave radiation is

$$Q_{L\uparrow} = \epsilon_m \sigma T_s^4 \quad (20)$$

where  $\epsilon_m$  is the water emissivity equal to 0.97,  $\sigma$  the Stefan-Boltzmann constant equal to  $5.67 \cdot 10^{-8} (\text{Wm}^{-2} \text{K}^{-4})$ .

The major problem in determining the net long wave radiation is to get a proper estimate of the incoming long wave radiation ( $Q_{L\downarrow}$ ). In this study Brunt's formula modified with a cloud factor according to Washington et al (1976) is used. It then reads

$$Q_{L\downarrow} = \sigma T_a^4 (c+d(e_a)^{0.5})(1+hN) \quad (21)$$

where  $c$ ,  $d$  and  $h$  are empirical coefficients equal to 0.67, 0.05 and 0.25 respectively,  $e_a$  is the atmospheric water vapour pressure (mb),  $N$  the total cloud cover in tenths and  $T_a$  the air temperature.

The sensible and latent heat flux formulations are taken from Friehe and Schmitt (1976). They used bulk aerodynamic formulas for the sensible heat flux ( $Q_C$ ) and the latent heat flux ( $Q_E$ ) according to

$$Q_C = \rho_a C_p^a C_C |\bar{V}^a| (T_s - T_a) \quad (22)$$

$$Q_E = LC_E |\bar{V}^a| (Q_s - Q_a) \quad (23)$$

where  $\rho_a$  is the air density,  $C_p^a$  specific heat at constant pressure for the air,  $C_C$  and  $C_E$  heat transfer coefficients,  $|\bar{V}^a|$  mean wind speed,  $L$  latent heat of evaporation,  $Q_s$  and  $Q_a$  water vapour densities at the sea surface and the atmosphere respectively. The heat transfer coefficients  $C_C$  and  $C_E$  are put equal to  $1.41 \cdot 10^{-3}$  and  $1.32 \cdot 10^{-3}$  respectively. Measurements of  $Q_s$  and  $Q_a$  are not directly available why a transformation to the water vapour pressure ( $e_s$ ) and ( $e_a$ ) was done. Under the assumption that the air close to the sea surface is saturated and has the same temperature as the sea surface,  $e_s$  is only a function of the sea surface temperature. The water vapour pressure in the air,  $e_a$ , is a function of both air temperature and relative humidity. Based upon humidity data from Bjuröklubb the relative humidity is put constant equal to 90%.

Within above assumptions, the surface heat budget equation (18) can be solved just knowing wind velocity, air temperature, water temperature and cloud amount.

Apart from the surface heat fluxes the wind stress,  $\tau$ , on the water surface had to be calculated. Generally a quadratic stress law is used

$$\tau = \rho_a C_d |\mathcal{V}^a| \mathcal{V}^a \quad (24)$$

where  $\mathcal{V}^a$  is the wind velocity at 10 meters above sea surface and  $C_d$  the wind drag coefficient. In general it is a function of the wind and the stability but in this study a constant drag coefficient, equal to  $1.3 \cdot 10^{-3}$ , is used.

#### 4. MODEL ILLUSTRATIONS

##### 4.1 Introduction

Before analysing the cooling of the Bay of Bothnia some simplified calculations are presented to illustrate the model with special emphasis on changes in water temperatures.

The presence of salinity in the Bay of Bothnia causes great difference compared with lakes. Neglecting salinity effects the model describes temperature changes in a lake. Note, however, that pressure effects on density and temperature of maximum density are neglected in this paper, see Farmer and Carmack (1981). For constant net heat loss of  $200 \text{ Wm}^{-2}$ , constant area versus depth and a constant wind of  $5 \text{ ms}^{-1}$  the solution becomes according to figure 6.

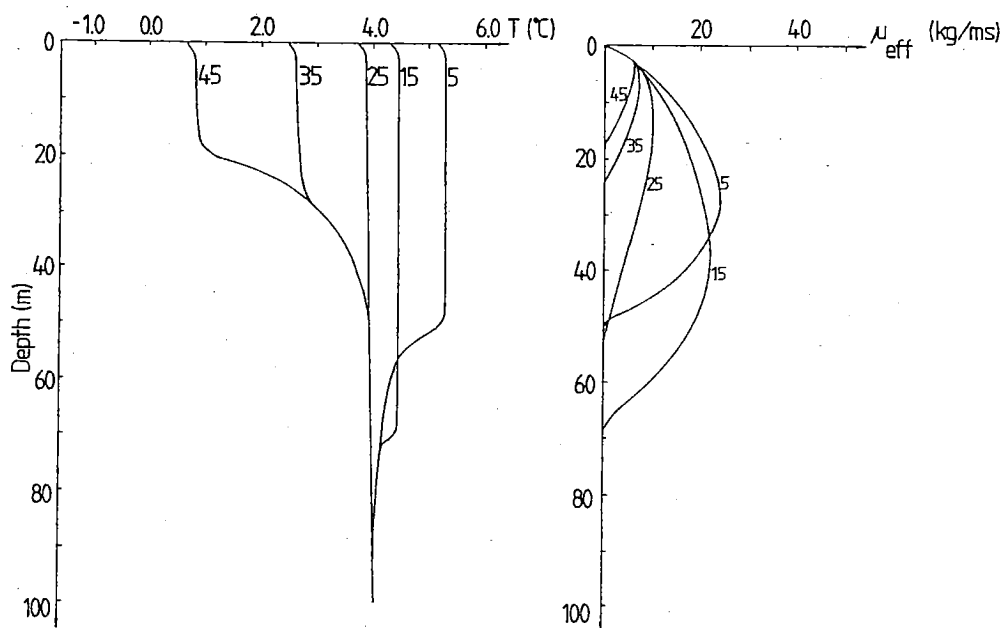


Figure 6 Cooling in a lake during idealized conditions. The wind velocity is  $5 \text{ ms}^{-1}$  and the net heat loss  $200 \text{ Wm}^{-2}$ . The numbers at the curves are day numbers.

From the computed temperature profiles one can see how the fresh water mass first is cooled down to the temperature of maximum density, which is close to 4°C. The whole water column, down to the bottom, reaches this temperature and further cooling leads to re-stratification. This speeds up the cooling rate of the surface water and cooling down to freezing point can be rather fast, particularly if the wind is weak.

Turbulent exchange in the water is illustrated by the right diagram in figure 6. The dynamic eddy viscosity values ( $\mu_{eff}$ ) represent how effective the turbulent processes are. Large values, due to convection and shear, are calculated before the temperature of maximum density is reached. After this the buoyancy flux changes sign and restratification starts reducing the turbulent exchange.

#### 4.2 Cooling of brackish sea water

If the water is saline some additional processes become important for the cooling rate. In this chapter initial profiles of salinity and temperature is used according to figure 7 and the variation of horizontal area versus depth is in accordance with the Bay of Bothnia.

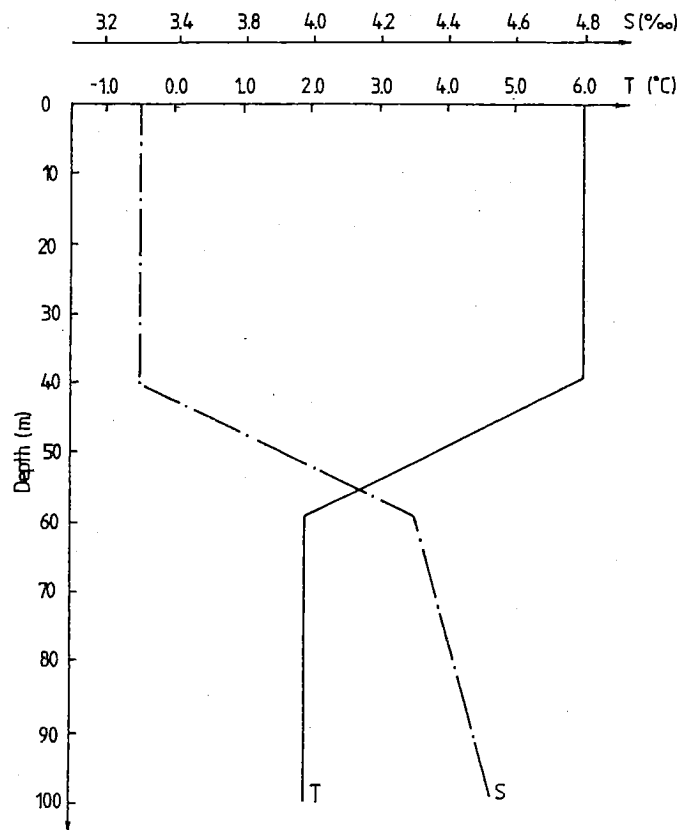


Figure 7 Initial profiles of temperature (T) and salinity (S) for the model illustrations.

Figure 8 illustrates cooling of brackish sea water in a basin corresponding to the Bay of Bothnia with a constant net heat outflow of  $200 \text{ Wm}^{-2}$  and a wind speed of  $5 \text{ ms}^{-1}$ . Two most important differences compared to figure 6 are that the temperature for maximum density is now lowered down to  $3.2^\circ\text{C}$  and that the halocline inhibits convection down to the bottom. The salinity profile also reduces the deepening rate of the wind mixed layer which could for example be seen in equation 10, where a stable salinity gradient always works as a sink in the turbulent kinetic energy equation and therefore reduces the turbulent exchange. From figure 8 it is also seen a negative temperature gradient just below the well mixed layer. This is possible as the salinity gradient stabilizes the density profile.

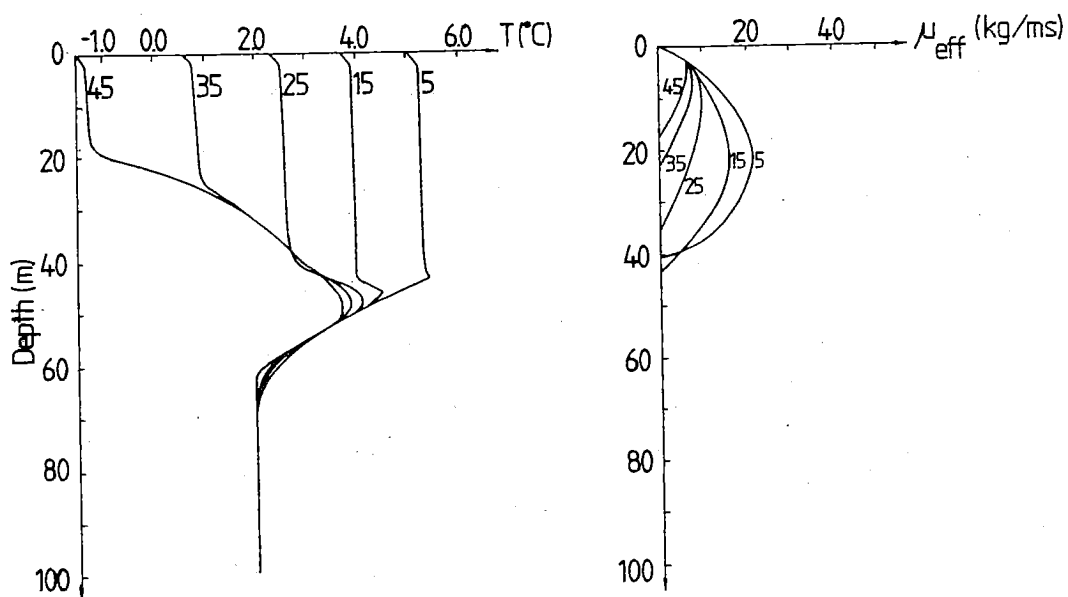


Figure 8 Cooling of brackish sea water during idealized conditions. The wind velocity is  $5 \text{ ms}^{-1}$  and the net heat loss  $200 \text{ Wm}^{-2}$ . The numbers at the curves are day numbers.

Meteorological forcing is however most changeable. To illustrate the importance of wind mixing on the cooling rate, calculations were made for zero wind speed and wind speeds of  $15 \text{ ms}^{-1}$ , figure 9. The net heat outflow is as before  $200 \text{ Wm}^{-2}$ . The figure 9 should be compared with figure 8. Due to the wind, the mixed layer differs

considerably. This highly effects the cooling rate. One could for example see that cooling down to freezing point during zero wind condition takes about 25 days. If the wind speed is  $15 \text{ ms}^{-1}$ , the freezing temperature is not reached even after 45 days..

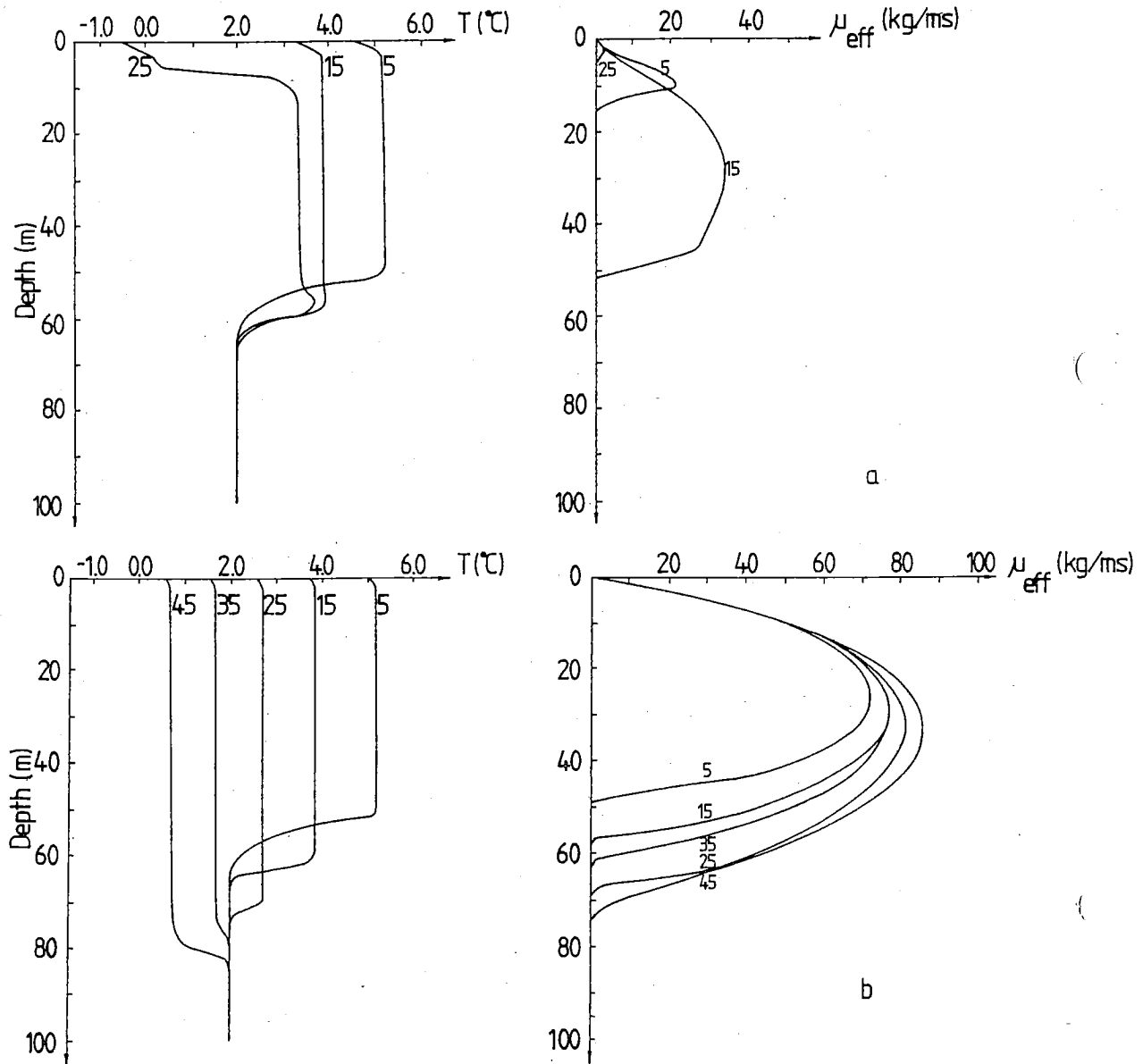


Figure 9 Cooling of brackish sea water during idealized conditions. In a) the wind velocity is  $0 \text{ ms}^{-1}$  and in b) the wind velocity is  $15 \text{ ms}^{-1}$ . The net heat loss is  $200 \text{ Wm}^{-2}$ . The numbers at the curves are day numbers

#### 4.3 Different eddy viscosity assumptions

A main problem in modelling the mixed layer is to represent the turbulent processes in a physical way. One classic approach to

this problem was made by Ekman (1905). Ekman used a constant vertical exchange coefficient when he studied the influence of the earth's rotation on ocean currents. Later work has proposed eddy diffusion coefficients of different forms. For example Madsen (1977) pointed out that an eddy viscosity coefficient which increases linearly from the sea surface is a more realistic model for the wind induced Ekman boundary layer. From observations in the Baltic, Kullenberg (1976) studied the vertical mixing in the surface layer of the sea. In his work just conditions with fairly strong winds and stable stratified waters were treated. During cooling both stable and unstable condition must be considered, and therefore the complete turbulent kinetic energy equation must be solved.

Figure 10 illustrates how important different assumptions on the eddy viscosity are for the cooling rate. In figure 10 a, b and c the net heat outflow is  $200 \text{ Wm}^{-2}$  and the wind speed is  $5 \text{ ms}^{-1}$  but different eddy viscosity formulations are used. Figure 10 a illustrates a constant dynamical eddy viscosity coefficient which increases linearly with depth in the upper surface layer, but is constant in the main water column. The calculated temperature profiles are completely unrealistic compared with temperature profiles in the Bay of Bothnia. In figure 10 b also a constant dynamical eddy viscosity coefficient is assumed which increases linearly close to the sea surface and is constant just down through the well mixed layer. The calculated temperature profiles seem a little more realistic but the negative temperature gradient just below the well mixed layer is too exaggerated and the solution also disregards the dynamics of the turbulent processes. In figure 10 c the solution is in accordance with the model presented in this paper.

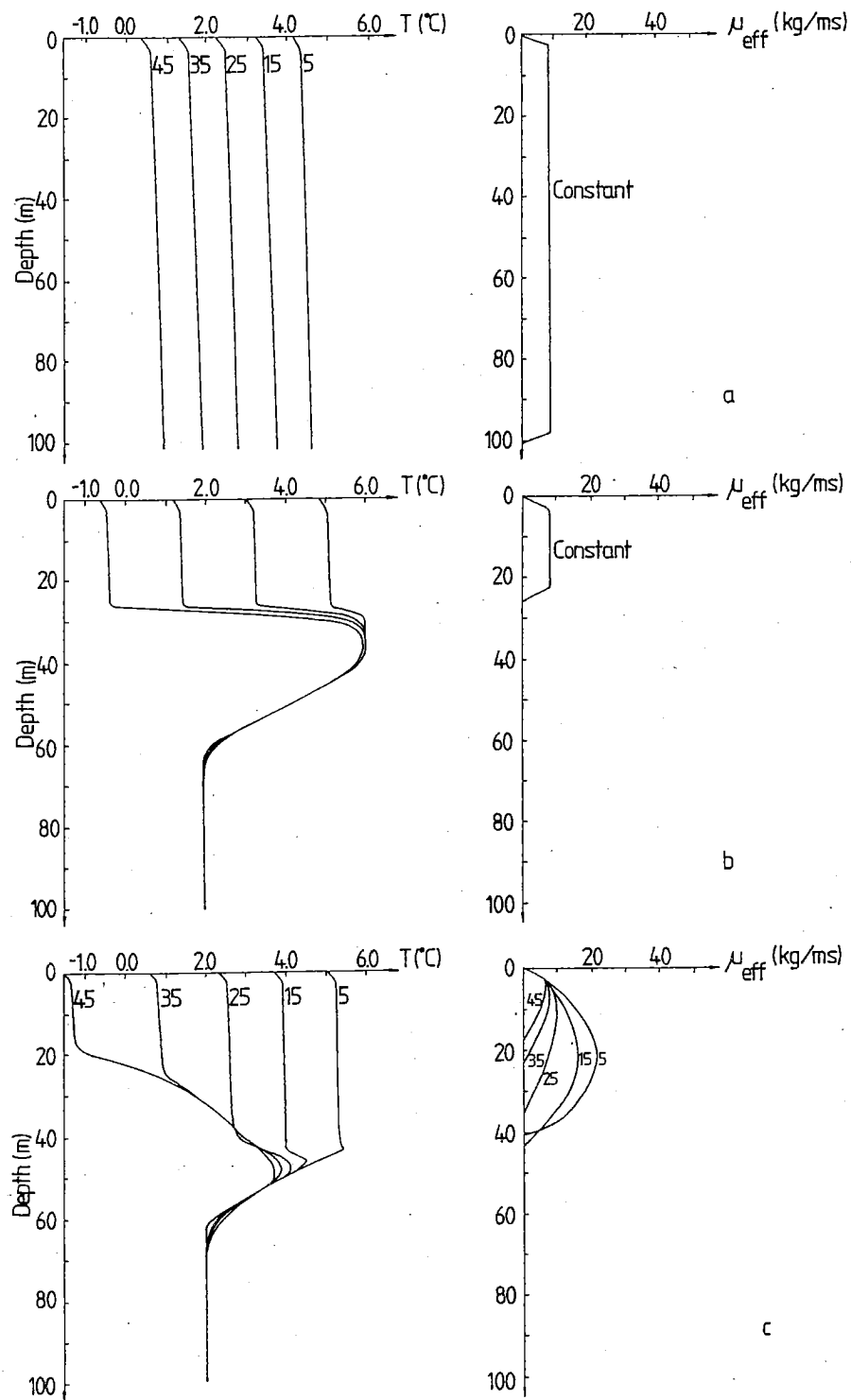


Figure 10 Cooling of brackish sea water with different turbulent models. In all cases the wind speed is  $5 \text{ ms}^{-1}$  and the net heat loss is  $200 \text{ Wm}^{-2}$ . The numbers at the curves are day numbers.

## 5. MODEL APPLICATION TO THE BAY OF BOTHNIA

### 5.1 Water temperature data

On October 22, 1979 a water temperature measuring system was placed in the Bay of Bothnia, see figure 11. The system contained two thermistor chains, type Aanderaa, with 11 thermistors in each. The water temperature was measured from a depth of 1 m below the sea surface to a depth of 75 m. The vertical resolution was 2 m for the upper chain and 5 m for the lower chain. Temperatures were measured every 30 minutes and stored on a magnetic tape. The relative accuracy of the data is better than  $0.05^{\circ}\text{C}$ . Due to the risk of ice formation the experiment ended at December 14. The temperature system had then been working for 52 days and fortunately no data were lost.

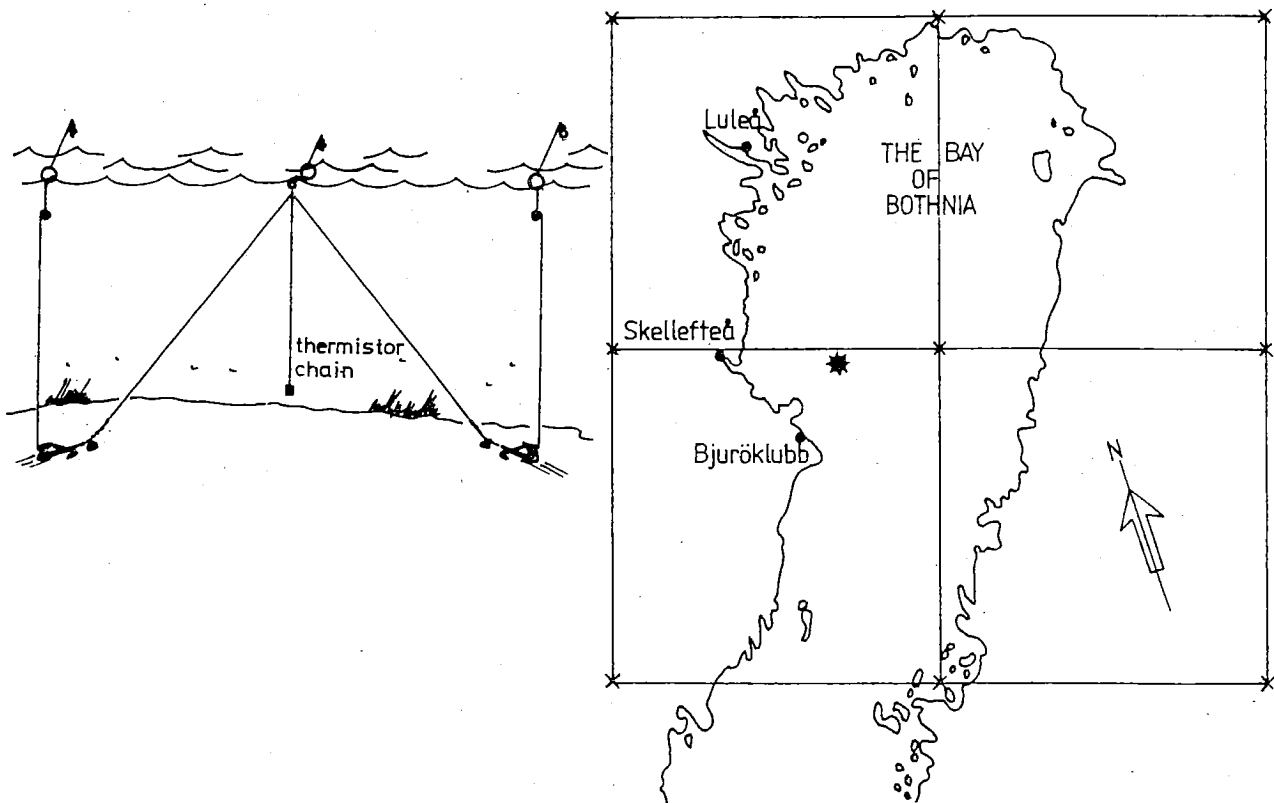


Figure 11 Map over the Bay of Bothnia with the 150 km meteorological grid given by the crosses. The position of the temperature measurements is indicated by the star. The measuring system is shown schematically beside the map.

To get a first insight in how the water was cooled during the period, changes in heat content were calculated from observed temperature data. In figure 12 the heat content in the upper 50 meters and in the deeper layer are plotted separately. The upper layer is influenced by meteorological forcing and therefore the heat content decreases during the cooling. The deeper water layer on the other hand shows a slight increase in the heat content. This is probably due to advective currents and could not be predicted by a one-dimensional theory. From figure 12 it is also seen a rather rapid change in heat content between November 8 to 14. This change is seen in all temperature data which indicate that advective currents could be important during this period.

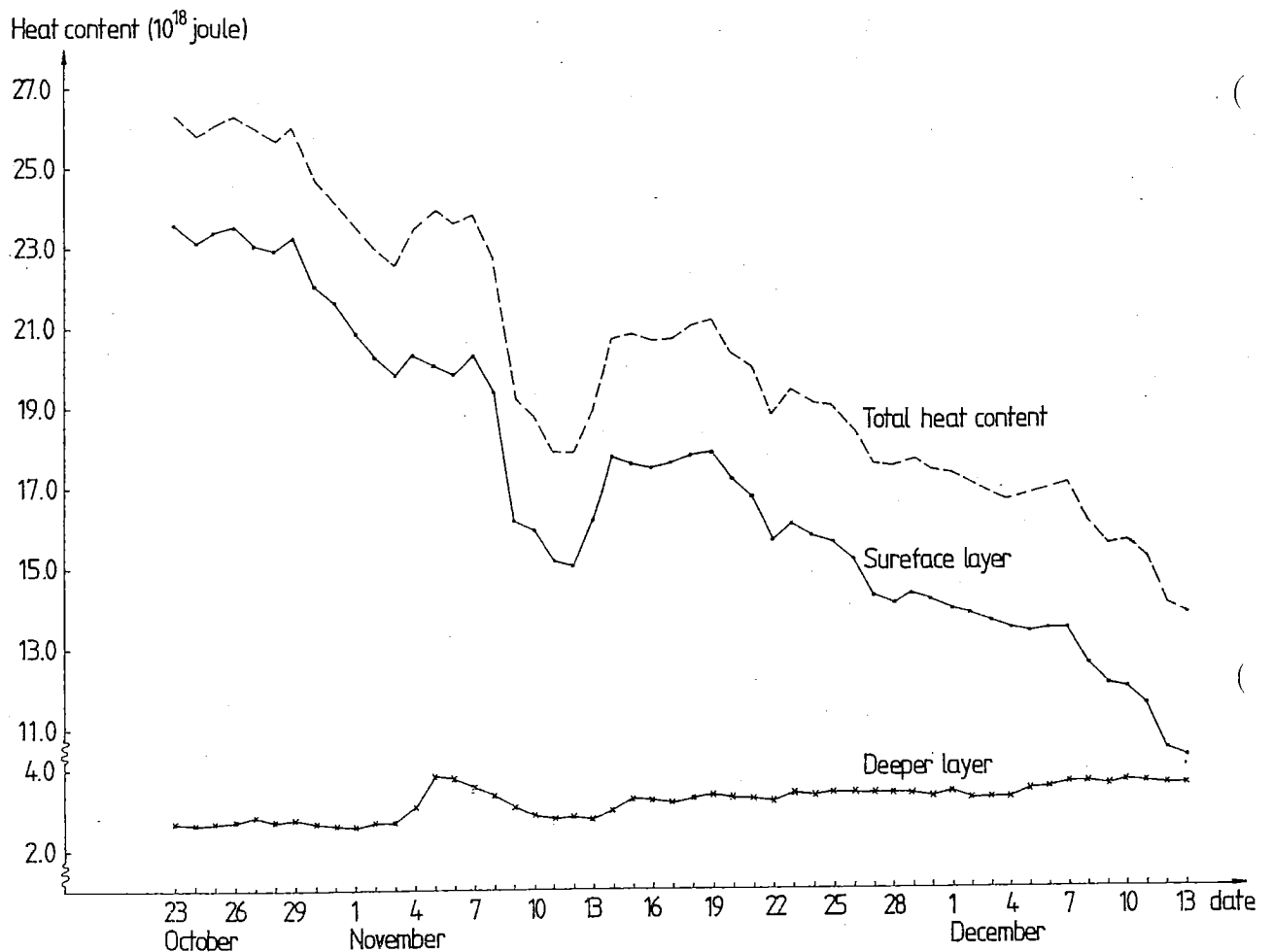


Figure 12 Heat content in the Bay of Bothnia based on the thermistor chain.

In the upper layer of the sea it is also interesting to study how the vertical temperature profiles vary during autumn cooling. In figure 13, the measured temperatures are plotted as 24 hours mean values for the whole period. The figure shows several interesting features. The temperature profiles start with a pronounced thermocline. During cooling a negative temperature gradient is reached.

Further cooling deepens the mixed layer and at the temperature of maximum density the temperatures are almost constant with depth in the surface layer. Passing the temperature of maximum density re-stratification starts in the surface layer and the well mixed depth is reduced.

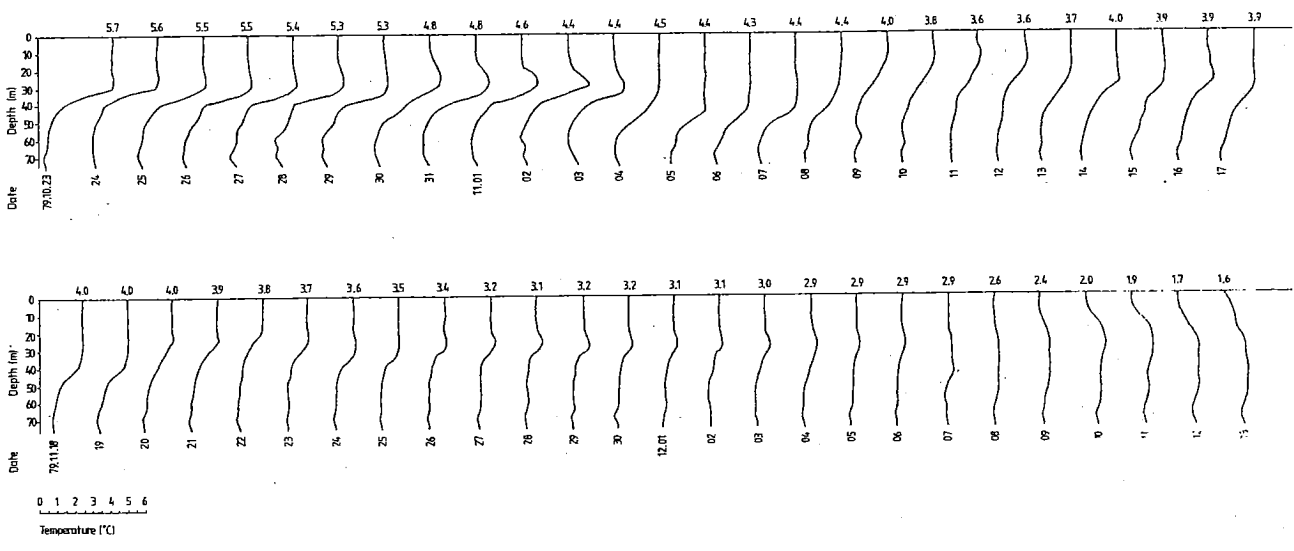


Figure 13 Measured temperature profiles, represented as 24 hour mean values.

### 5.2 Meteorological data

To calculate the heat and radiation fluxes and the wind stress, weather data have been extracted from analysed synoptic weather charts. This was done every third hour in a 150 km cartesian grid, see figure 11. Air temperature and air surface pressure data were extracted from nine grid points. The cloudiness was extracted as an areal average over the whole Bay of Bothnia. The grid used here is the same as the grids used in the routine weather models. In the future it will therefore be easy to couple the cooling model with a routine weather forecast model. The geostrophic wind speed was calculated from the extracted air pressure data. Together with areal mean temperatures and cloud coverage values net heat flux and wind stress were calculated according to chapter 3.5. Mean

values of the meteorological data are shown in figure 14.

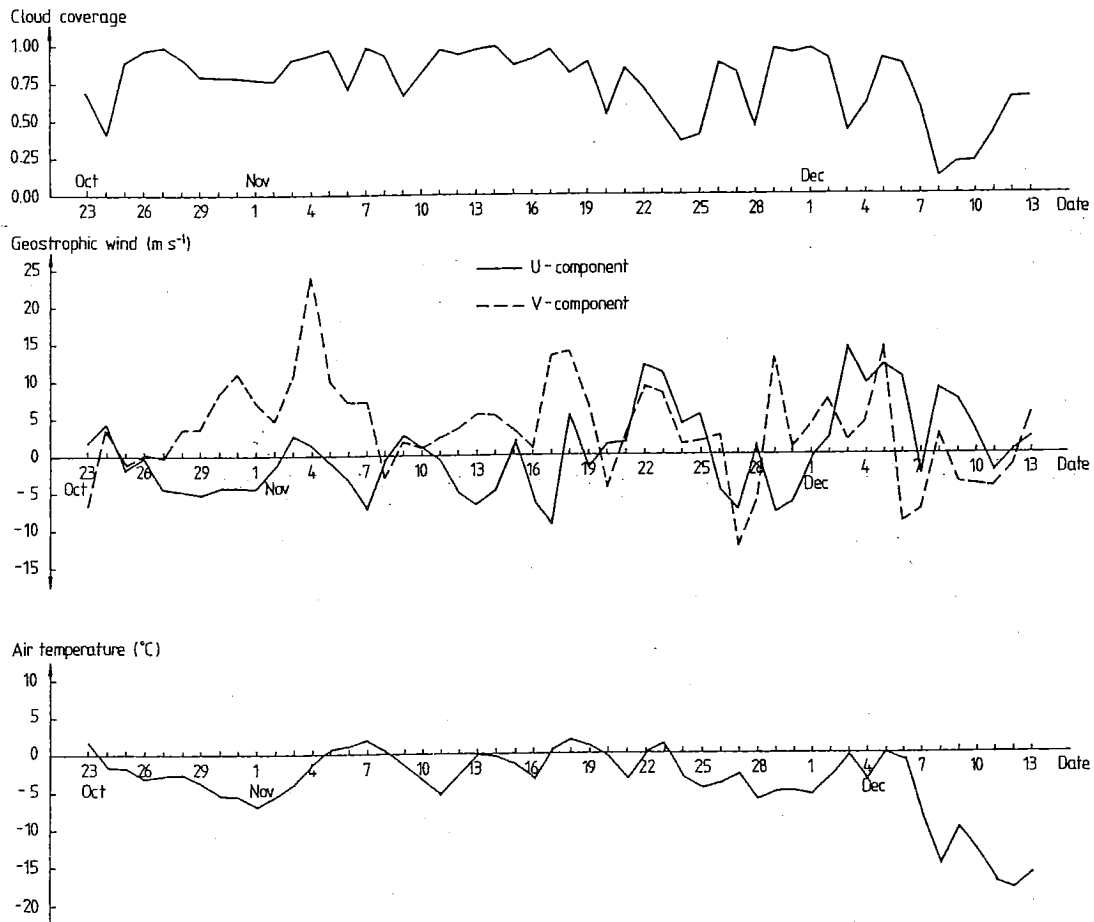


Figure 14 Meteorological data.

### 5.3 Comparison between calculated and observed temperatures

In this section the results of the field measurements and computations with the mathematical model will be presented. The model calculated the water temperatures with just initial profiles in salinity and temperature and with meteorological input data according to synoptic weather charts. Boundary conditions for the mathematical model were obtained as described in the previous section. Starting profiles in temperature and salinity is shown in figure 15, where the salinity profile is in accordance with an observation made by the Swedish Coast Guard close to the temperature system.

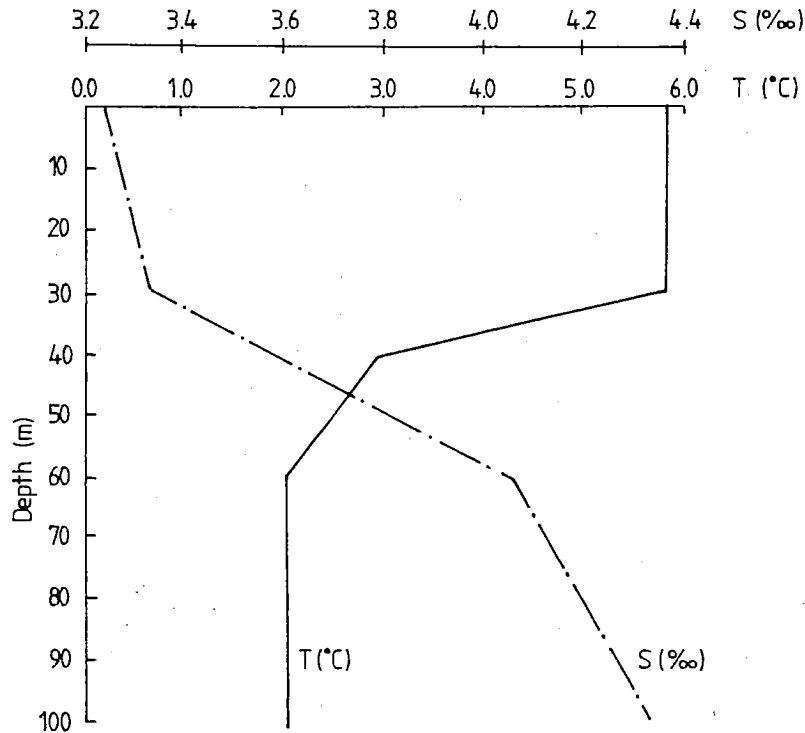


Figure 15 Initial profiles of temperature (T) and salinity (S) based upon measurements from October 23, 1979.

Computed and observed temperature profiles are compared in figures 16 and 17. In general there is a very good agreement between model results and observations. The deepening of the thermocline due to wind mixing and convection and the development of the restratification are well calculated.

The interest is now focused on details of measured and predicted temperature profiles. Figure 18 shows profiles of measured temperature (dashed line) and calculated profiles of temperature (T), salinity (S), density ( $\sigma_T$ ) and dynamical turbulent viscosity ( $\mu_{eff}$ ).

The first profile to be examined is the one on October 28. It is clear that both the measured and the predicted profile have a temperature maximum below the well mixed layer due to the combined effect of temperature and salinity gradients which cause stable stratification. During the next few days the model seems to be more sensitive to the increased wind stress and cooling than the measured profiles. In the model the temperature maximum below the well mixed layer is eroded faster than shown in the observed data.

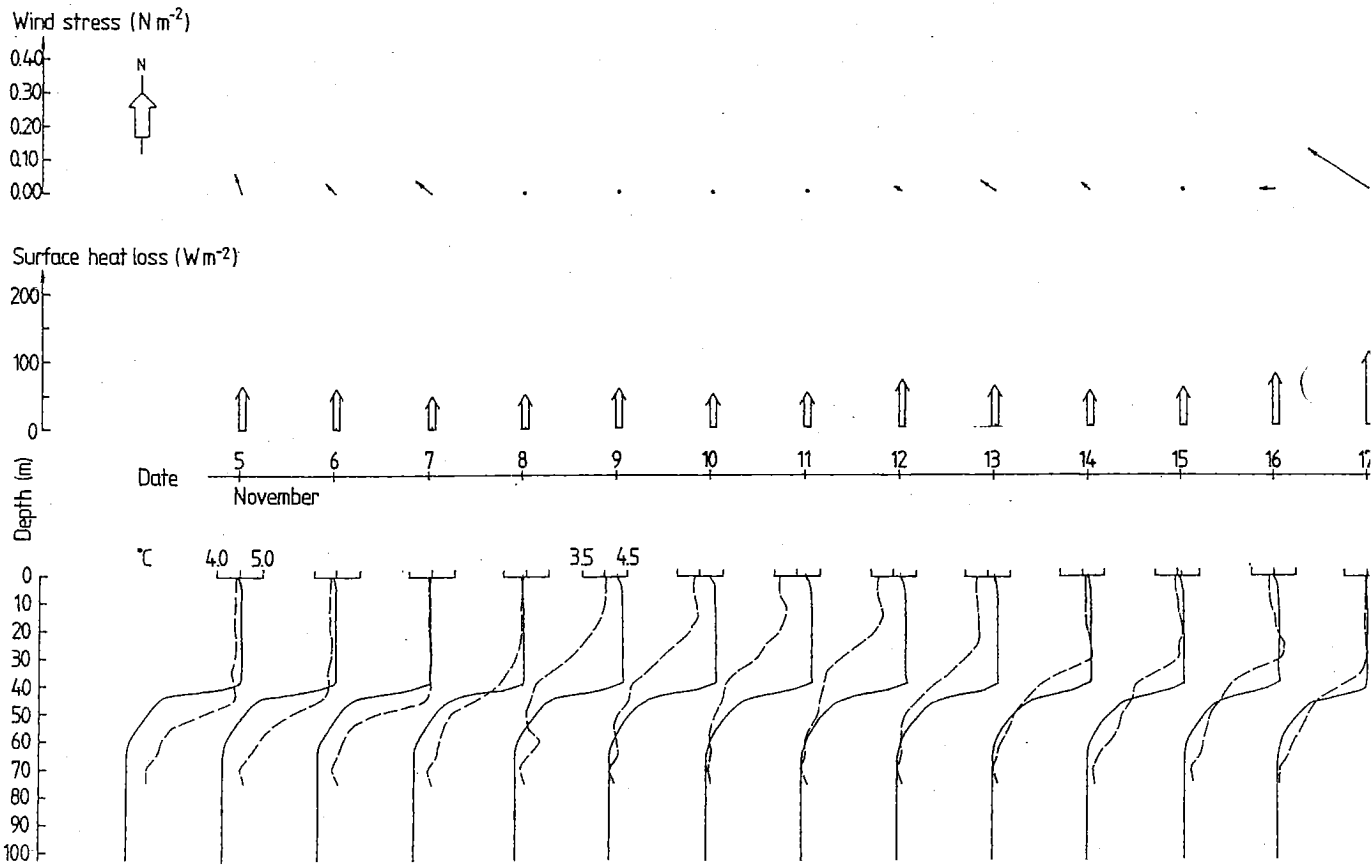
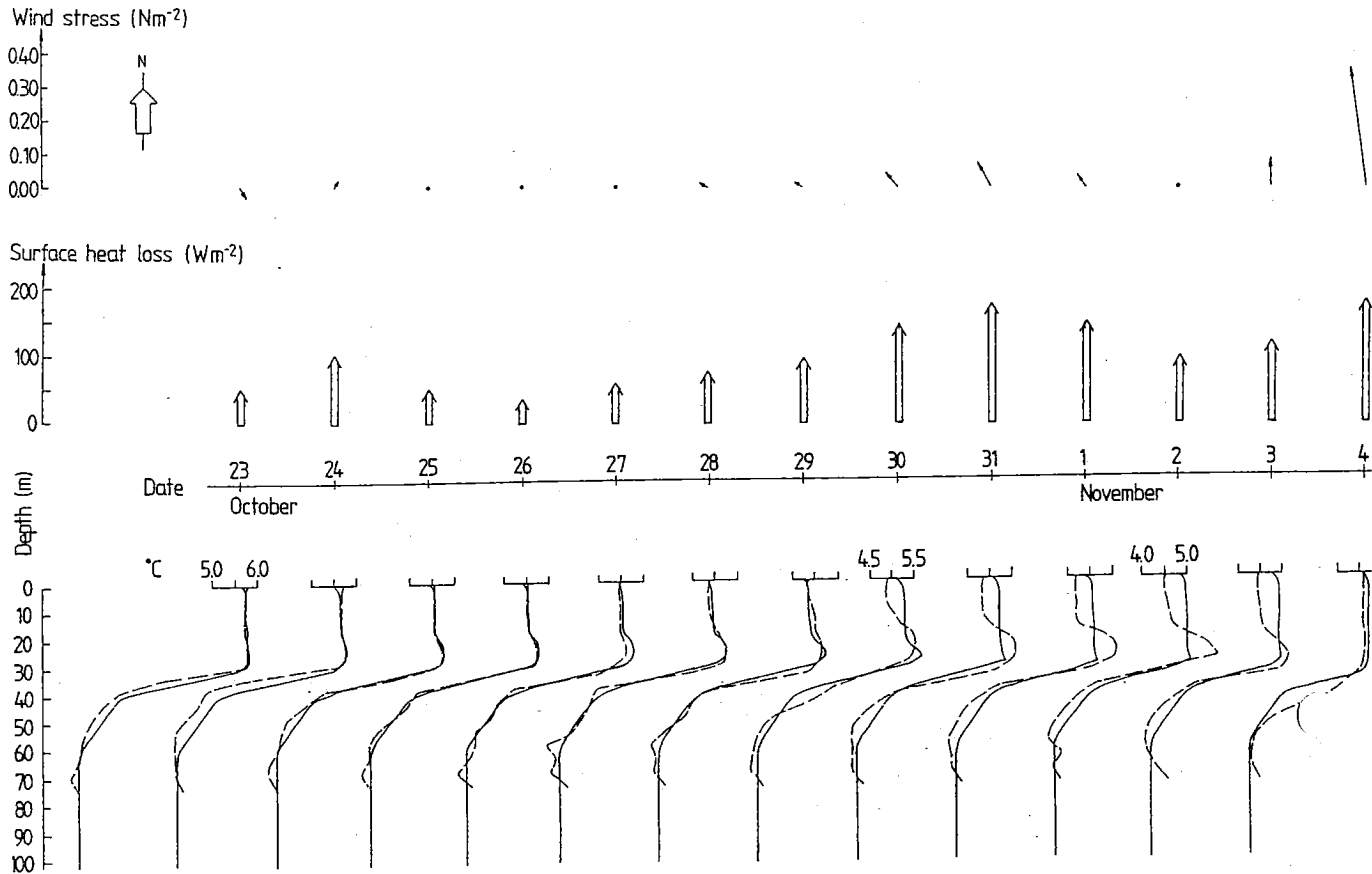


Figure 16 Calculated wind stresses, heat losses and results of the model run during the first 26 days, compared with observed temperature data (dashed line). All data are 24 hours mean values.

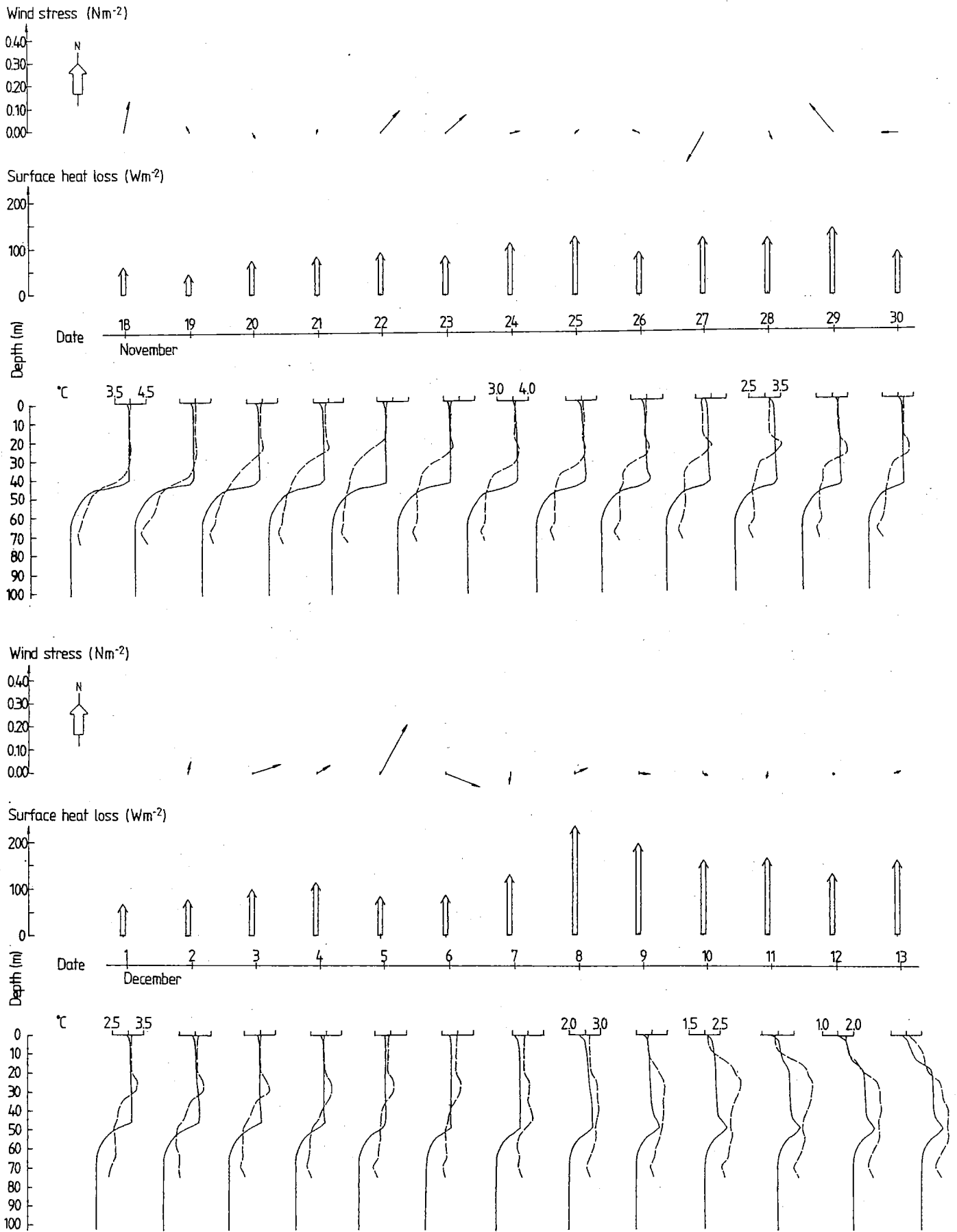


Figure 17 Calculated wind stresses, heat losses and results of the model run during the last 26 days, compared with observed temperature (dashed line). All data are 24 hours mean values.

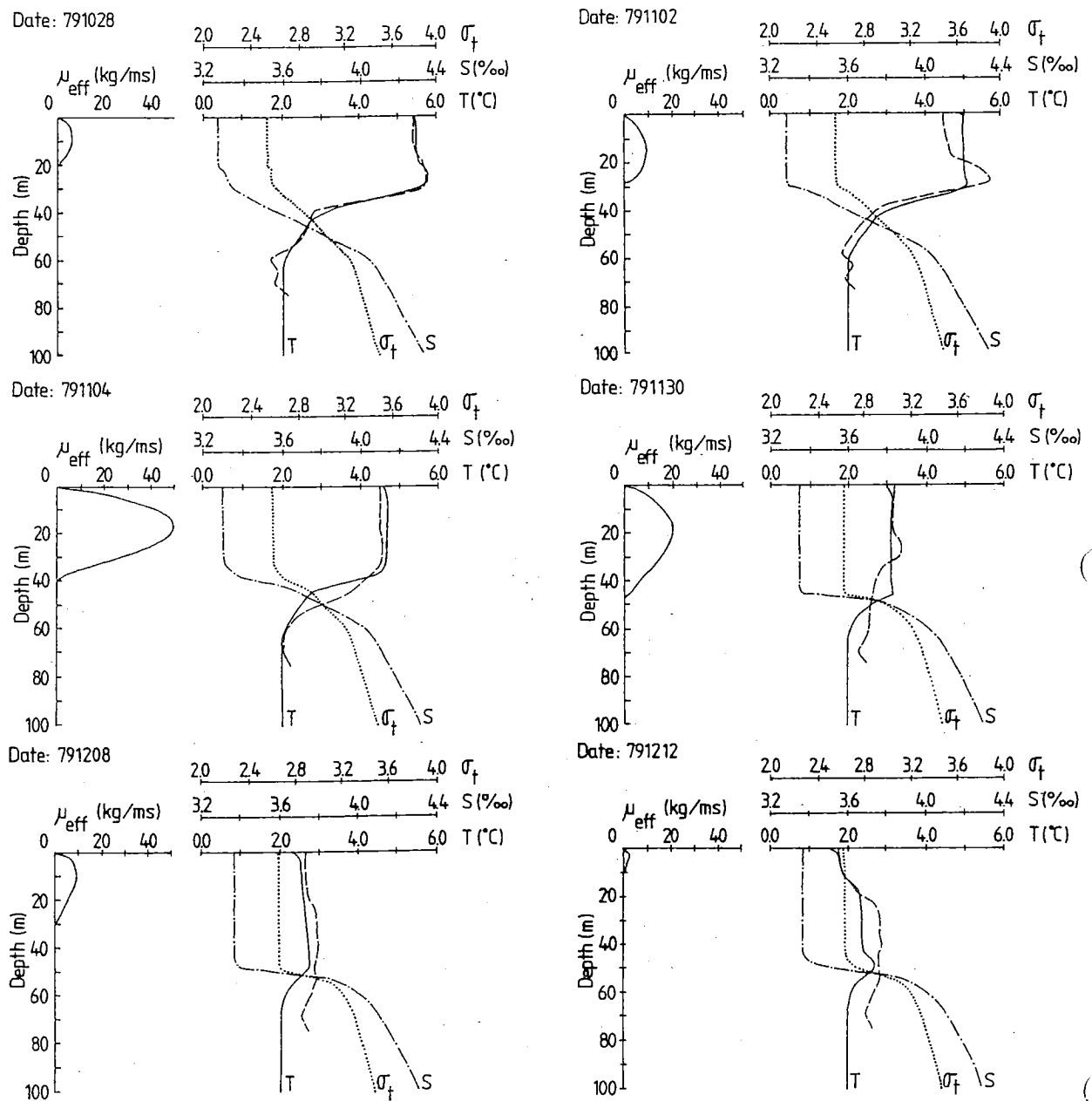


Figure 18 Model calculations of dynamical eddy viscosity ( $\mu_{eff}$ ), temperature ( $T$ ), salinity ( $S$ ) and density ( $\sigma_t$ ) for six occasions during the cooling period. The dashed lines are the observed water temperatures. All data are 24 hours mean values.

As no sinks and sources exist in the salinity equation and as advection is neglected, a much better result cannot be expected.

November 2 the depth of the well mixed layer is over predicted but two days later there is a strong wind and the depth of the mixed layer is again in good agreement with measurements. Details of these two days is found in figure 18.

A less encouraging period starts on November 9 and lasts for about five days. The cause of the disagreement might be traced by noting the rapid change of total heat content of the water column from November 7 to 9. The change is not caused by the surface heat flux. Advective transports are thus the only explanation. In figure 19 the explanation is firmly supported. It is seen that the change in the heat content by net surface heat flux does not correspond to actual change in heat content during the period. Actually, a diagram like this points out periods of strong advective influence, periods when one dimensional models are inadequate. The next date to pay particular attention to is November 30, since the mixed layer temperature now passes the temperature of maximum density,  $3.2^{\circ}\text{C}$ . Further cooling causes restratification. In figure 18 the mixed layer depth is almost 50 m as compared to 20 m on October 28. The temperature of the mixed layer is still correctly predicted even if the measured profile is not as straight as the one predicted. In December both temperature and salinity gradients act to reduce the mixing. December 8 and 12 are displayed in more detail in figure 18. The eddy viscosity profiles show that the fully turbulent layer is much more shallow than what could be concluded from the density profiles. The weak stable stratification due to the temperature is giving this effect. Interesting enough, these conditions are favourable for once again producing a maximum in temperature below the mixed layer. During the last days of the period the maximum is found both in measurements and predictions.

Presumably the examination of the particular profiles has demonstrated that cooling of brackish sea water brings out a number of interesting phenomenon. When judging the performance of the mathematical model one ought to have in mind the importance of salinity on density, that just initial profiles in temperature and salinity are used and also the inevitable uncertainty in the boundary conditions. In light of this the agreement obtained after 52 days of

integration is, in the authors view, most satisfactory.

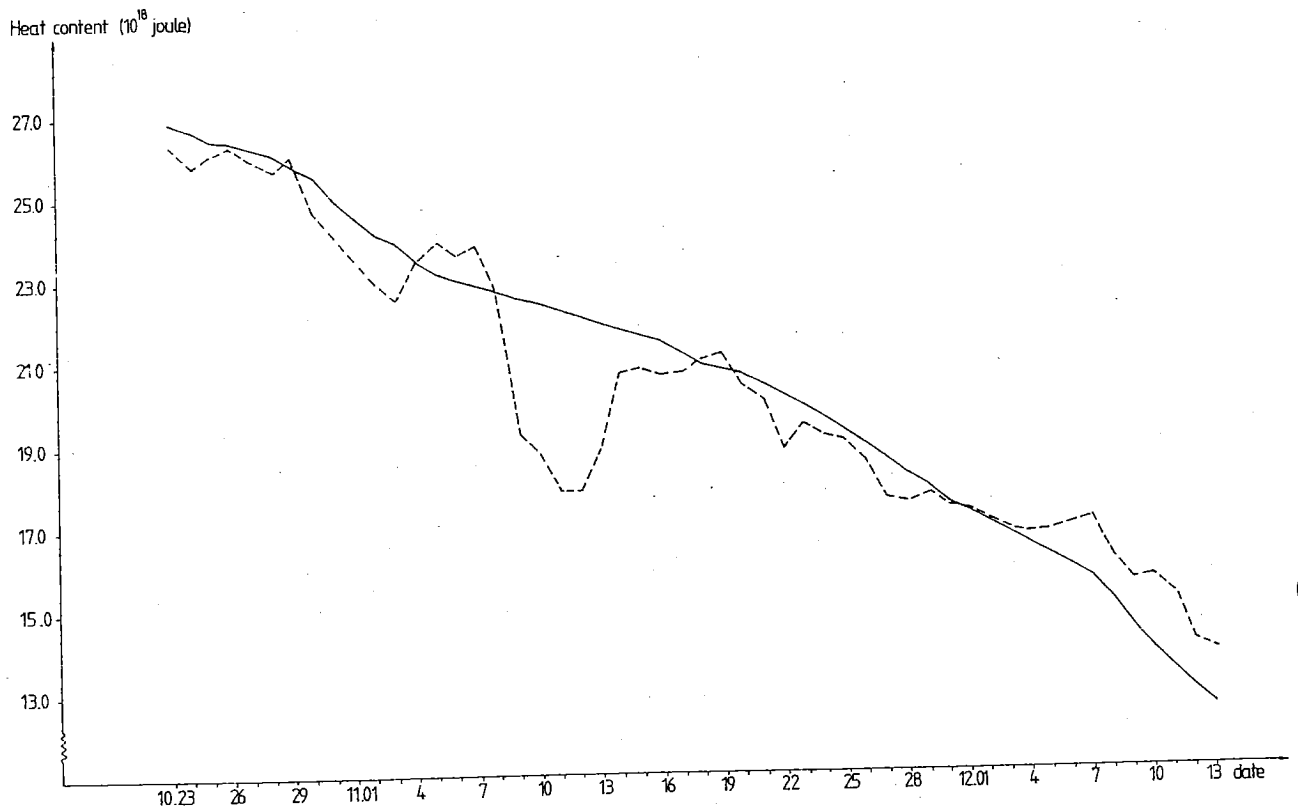


Figure 19 Heat content of the water column as given by the thermistor chain (dashed line) and expected variations due to the one-dimensional model (solid line).

## 6. SUMMARY AND CONCLUSIONS

The objective of this study was to examine cooling of the Bay of Bothnia during autumn. For this purpose temperature profiles were measured in the Bay of Bothnia during 52 days, from October 23 to December 13, 1979. The measured profiles have been compared to calculated ones, obtained by a mathematical model. The mathematical model is based on the conservation equations for momentum, heat and salt in their one-dimensional form and with an equation of state which is linear with respect to salinity and quadratic with respect to temperature. Turbulent exchange coefficients are calculated with a kinetic energy-dissipation model of turbulence.

It was demonstrated by the model that salinity influences the cooling by lowering the temperature for maximum density and that a stable salinity gradient reduces the deepening rate of the wind

mixed layer and inhibits convection down to the bottom. This salinity effects are of great importance when modelling cooling in the Bay of Bothnia.

The measured temperature profiles clearly demonstrate the importance of both temperature and salinity gradients in the mixed layer dynamics during autumn cooling.

Most important factors for the cooling rate are the heat loss at the air-sea interface and the mixing depth. The mixing depth depends mainly on wind mixing, convection and restratification when cooling has passed the temperature of maximum density. All these processes could well be described by the mathematical model and the computed and observed temperatures therefore agreed well.

During five days, advective effects were found to have a strong influence on the measured temperatures. Such events show the weakness of one-dimensional models, which of course cannot handle advection.

To test the model further temperature data have been collected at two locations in the Sea of Bothnia during 1981/82. If the results from these measurements are successful and model calculations are in as good agreement with measurements as above, an operational model for calculating cooling of sea water in the Bay and Sea of Bothnia is planned.

## Acknowledgements

In this work we would especially like to thank Urban Svensson for a fresh introduction in turbulence models and for many suggestions and support.

We would also like to thank Svante Bodin, Anders Stigebrandt, Thomas Thompson, Ingemar Udin and Wayne Wilmot for criticism and suggestions.

The excellent temperature measurements were possible to make due to assistance from the Swedish Administration of Shipping and Navigation and from Robert Hillgren, Bo Juhlin and Mats Moberg at SMHI.

All figures were drawn by Anita Bergstrand and Gun-Britt Rosén and the typing was made by Monika Johansson. Their help is gratefully acknowledged.

## Literature references

- Bodin, S (1979): A predictive numerical model of the Atmospheric Boundary Layer based on the Turbulent Energy Equation. SMHI-Rapporter, RMK 13 (1979), SMHI, Box 923, S-601 19 Norrköping, Sweden.
- Caldwell, D R (1978): The maximum density points of pure and saline water. Deep-Sea Research, 25, 175-181.
- Delnore, V E (1980): Numerical simulation of thermo-haline convection in the upper ocean. J Fluid Mech, vol 96, part 4, pp 803-826.
- Ekman, V W (1905): On the influence of the earth's rotation on ocean currents. Ark. f. Mat., Astron. och Fysik, vol 2, no 11, pp 1-53.
- Farmer, D M and E C Carmack (1981): Wind mixing and restratification in a lake near the temperature of maximum density. In press. J Phys Oceanogr.
- Friehe, C A and K F Schmitt (1976): Parameterization of Air-Sea Interface fluxes of Sensible Heat and Moisture by the Bulk aerodynamic Formulas. J of Phys Oceanography, 6, 801-809.
- Kondratyev, K (1969): Radiation in the atmosphere. International Geophysics Series, Vol 12, Academic Press, New York.
- Knudsen, M et al (1901): Hydrographic tables, G. E. C., Copenhagen.
- Kremling, K (1972): Comparison of specific gravity in natural sea water from hydrographical tables and measurements by a new instrument, Deep-Sea Research 19, pp 337-383.

- Kullenberg, G (1976): On vertical mixing and the energy transfer from the wind to the water. *Tellus* 28, pp 159-165.
- Launder, B E and D B Spalding (1972): *Mathematical models of turbulence*. Academic Press, London and New York, 1972.
- Madsen, O S (1977): A realistic model of the wind induced Ekman boundary layer. *J of Phys Oceanography*, Vol 7, pp 248-255.
- Mc Donald, J E (1960): Direct absorption of solar radiation by atmospheric water vapor. *J of Met*, Vol 17, pp 319.
- Miller, J R (1976): The Salinity Effect in a Mixed Layer Ocean Model. *J Phys Oceanogr*, 6, 29-35.
- Millero, F J and K Kremling (1976): The densities of Baltic Sea waters. *Deep-Sea Research*, Vol 22, pp 1129-1138.
- Niiler, P I and E B Kraus (1977): One-dimensional models of the upper ocean. In *Modelling and Prediction of the Upper Layers of the Ocean*, E B Kraus, Editor, Pergamon Press, 143-172.
- Pandalfo et al (1971): Prediction by numerical models of transport and diffusion in an urban boundary layer. The Center for the Environment and Man.
- Rodi, W (1980): Turbulence models and their application in hydraulics - a state of the art review. Presented by the IAHR-Section on Fundamentals of Division II: Experimental and Mathematical Fluid Dynamics, Secretariat: Rotterdamseweg 185 - P O Box 177, 2600 MH DELFT, The Netherlands.

Sahlberg, J and H Törnevik (1980): A study of the large scale cooling in the Bay of Bothnia. SMHI-Rapporter, RMK 22 (1980). SMHI, Box 923, S-601 19 NORRKÖPING, Sweden.

Singhal, A K and D B Spalding (1981): Predictions of two-dimensional boundary layers with the aid of the  $k-\epsilon$  model of turbulence. Computer Methods in Applied Mechanics and Engineering 25 (1981), 365-383.

SMHI and FIMR (1982): Climatological ice atlas for the Baltic Sea, Kattegat, Skagerrak and Lake Vänern (1963-1979). Swedish Met. and Hydr. Institute (SMHI) and Finnish Institute of Marine Research (FIMR). 1982 in press.

Svensson, U (1978): A mathematical model of the seasonal thermocline. Report No 1002, Dept of Water Resources Eng, Univ of Lund, Sweden.

Svensson, U (1979): The structure of the turbulent Ekman layer. Tellus, 31, 340-350.

Svensson, U (1981): On the influence of buoyancy on the turbulent Ekman layer. Proc Symp on Turbulent Shear Flows. Univ of California, Davis.

Thompson, S T (1979): Development of a seasonally - verified Planetary Albedo parameterization for zonal energy balance climate models. Report of the IOC study conference on climate models: Performance, intercomparison and sensitivity studies. Global Atmospheric Research Programme (GARP) publications series no 22, Dec 1979, WMO.

Walín, G (1972): On the hydrographic response to transient meteorological disturbances. Tellus 24, 164-186.

Washington W M, Semtner A J, Parkinson C and L Morrison  
(1976): On the development of a Seasonal  
Change Sea-Ice Model. J of Phys Oceanography,  
6, 679-685.

## Nomenclature

<u>Symbol</u>	<u>Meaning</u>
$a_i$	constants
$A_w$	absorption function
$b_i$	constants
$C$	a constant
$C_{1\epsilon}, C_{2\epsilon}, C_{3\epsilon}, C_\mu$	constants in turbulence model
$C_p, C_p^a$	specific heat
$C_C, C_E$	heat transfer coefficients
$C_d$	drag coefficient
$d$	a constant
$e_a, e_s$	vapour pressure
$f$	coriolis parameter
$g$	gravitational acceleration
$h$	a constant
$k$	turbulent kinetic energy
$l$	length scale
$L$	latent heat of evaporation
$N_i$	amount of clouds of category $i$
$N$	total cloud coverage
$Q$	net heat flux
$Q_s$	net short wave radiation
$Q_L, Q_{L+}, Q_{L-}$	long wave radiation
$Q_C$	sensible heat flux
$Q_E$	latent heat flux
$Q_0$	solar constant
$Q_s, Q_a$	water vapour density
$S$	salinity
$T$	water temperature

<u>Symbol</u>	<u>Meaning</u>
$T_a$	air temperature
$T_f$	freezing point temperature
$T_u$	air turbidity
$T_i$	cloud function
$T_R$	transmission function
$T_s$	surface water temperature
$T_{\rho m}$	temperature for maximum density
$t$	time
$U$	mean wind velocity in x-direction
$V$	mean wind velocity in y-direction
$ \overline{V^a} $	mean wind velocity
$\overline{w_u}, \overline{w_v}$	Reynold stresses
$\overline{w\theta}, \overline{ws}$	turbulent transport of heat and salt
$Z$	vertical coordinate
$Z'$	zenith angle
$\alpha$	a constant
$\alpha'$	sea surface albedo
$\beta$	a constant
$\epsilon$	rate of dissipation of $k$
$\epsilon_m$	water emissivity
$\kappa$	molecular thermal diffusivity
$\kappa_s$	molecular diffusivity of salt
$\mu_{eff}$	effective dynamical eddy viscosity ( $\mu_{eff} = \rho \nu_T$ )
$\nu$	molecular kinematic viscosity
$\nu_T$	turbulent kinematic eddy viscosity
$\rho_a$	air density
$\rho, \rho_0$	water density
$\sigma$	Stefan Bolzmans constant

<u>Symbol</u>	<u>Meaning</u>
$\sigma_k, \sigma_\varepsilon, \sigma_T, \sigma_S$	Prandtl/Schmitt numbers
$\sigma_t$	water density ( $\rho=1000$ )
$\tau_x, \tau_y, \tau$	wind stresses

SWEDISH/FINNISH WINTER NAVIGATION

RESEARCH BOARD

R E P O R T S

- | No.  | Titel  |
|------|--|
| 1.   | HAVSISKONFERENS. Protokoll (1972).   |
| 2.   | VINTERSJÖFART I BOTTENHAVET - Erfarenheter av SCA:s distributionssystem - L. Sjöstedt och S. Hammarsten (1972).  |
| 3.   | ISSKADOR PÅ FARTYG I ÖSTERSJÖN, BOTTENHAVET OCH BOTTENVIKEN - Statistisk analys av skadefrekvenser - L. Sjöstedt och S Hammarsten (1973).  |
| 4.   | PROPELLERPROBLEM. Propellerverkningsgradens beroende av bladutformningen. H. P. Loid (1973).   |
| 5.   | FARTYGS FRAMDRIVNINGSMOTSTÅND I IS. E. Enkvist (1974).   |
| 6.   | VINTERSJÖFART MED STORA FARTYG I BOTTENVIKEN - Rapport av en arbetsgrupp. (1974).  |
| 7.   | VINTERSJÖFART I BOTTENVIKEN. Symposium i Luleå (1974).   |
| 8.   | HAVSISUNDERSÖKNINGEN I BOTTENVIKEN VINTERN 1974. A. Omstedt, T. Thompson och I. Udin (1974).   |
| 9.   | KARTERING AV YTVATTENTEMPERATUREN I VATTNEN RUNT SVERIGE. J-E. Lundqvist, A. Omstedt och I. Udin (1974).   |
| 10.  | EXPERIMENTS ON REMOTE SENSING OF SEA ICE USING A MICROWAVE RADIOMETER. M. Tiuri, M. Hallikainen and K. Kaski (1974).   |
| 11.  | BOTTENVIKENS STÅLFYRAR - HÅLLFASTHETSANALYS OCH FÖRBÄTTRINGSFÖRSLAG. M. Määttänen (1974).  |
| 12.  | FORMATION AND STRUCTURE OF ICE RIDGES IN THE BALTIC. E. Palosuo (1975).  |
| 13.  | CALCULATION OF ICE DRIFT IN THE BOTHNIAN BAY AND THE QUARK. A. Valli and M. Leppäranta (1975).   |
| 14.  | A NARROW BEAM SONAR TO MEASURE THE SUBMARINE PROFILE OF AN ICE RIDGE. E. Palosuo, T. Pousi and M. Luukkala (1976).   |
| 15.  | THE AVERAGE SURFACE TEMPERATURE IN THE AUTUMN AND THE EARLY WINTER ON THE GULF OF BOTHNIA, THE NORTHERN BALTIC SEA AND THE GULF OF FINLAND (1966-1974). H. Grönvall and E. Palosuo (1976). |
| 16:1 | SEA ICE -75. Programme. Å. Blomquist, C. Pilo and T. Thompson (1975).  |
| 16:2 | SEA ICE -75. Ground truth report. I. Udin (1976).  |
| 16:3 | SEA ICE -75. Ice detection by SLAR. R.H.J. Morra and G.P. de Loor (1976).  |
| 16:4 | SEA ICE -75. Analysis of SLAR data. S. Parashar (1976).  |
| 16:5 | SEA ICE -75. FLAR, ODAR, ship's radar. J. Nilsson, T. Hagman and Y. Nilsson (1976).  |

- 16:6 SEA ICE -75. IR-scanner results. E. Fagerlund and G. Lundholm (1976).
- 16:7 SEA ICE -75. Radaraltimeter results. S. Axelsson (1976).
- 16:8 SEA ICE -75. Dynamical report. I. Udin and A. Omstedt (1976).
- 16:9 SEA ICE -75. Summary report. Å. Blomquist, C. Pilo and T. Thompson (1976).
17. THE SHAPE AND SIZE OF ICE RIDGES IN THE BALTIC ACCORDING TO MEASUREMENTS AND CALCULATIONS. A. Keinonen (1976).
18. A NUMERICAL MODEL FOR FORECASTING THE ICE MOTION IN THE BAY AND SEA OF BOTHNIA. I. Udin and A. Ullerstig (1977).
19. CREEP OF FRESH WATER ICE AT HIGH HOMOLOGOUS TEMPERATURES. E.K.M. Leppävuori (1976).
20. ECONOMICS OF WINTER NAVIGATION IN THE NORTHERN PART OF THE GULF OF BOTHNIA. B.M. Johansson (1977).
21. MEASUREMENTS AND ANALYSIS OF ICE-INDUCED STRESSES IN THE SHELL OF AN ICEBREAKER. P. Varsta (1977).
22. MEASUREMENTS OF PHYSICAL CHARACTERISTICS OF RIDGES ON APRIL 14 AND 15, 1977. A. Keinonen (1977).
23. ICE ACCRETION ON SHIPS WITH SPECIAL EMPHASIS ON BALTIC CONDITIONS. J-E. Lundqvist and I. Udin (1978).
24. PRESENTATION OF SEA ICE RIDGES IN GENERAL AND PHYSICAL CHARACTERISTICS OF BALTIC RIDGES FOR SHIP RESISTANCE CALCULATIONS. A. Keinonen (1978).
25. ON CONDITIONS FOR THE RISE OF SELF-EXCITED ICE-INDUCED AUTONOMOUS OSCILLATIONS IN SLENDER MARINE PILE STRUCTURES. M. Määttänen (1978).
26. SOME RESULTS FROM A JOINT SWEDISH-FINNISH SEA ICE EXPERIMENT, MARCH 1977. A. Omstedt and J. Sahlberg (1978).
27. ON PLASTIC DESIGN OF AN ICE-STRENGTHENED FRAME. P. Varsta, I.V. Droumev and M. Hakala (1978).
28. LONG TERM MEASUREMENTS OF ICE PRESSURE AND ICEINDUCED STRESSES ON THE ICE BREAKER SISU IN WINTER 1978. J. Vuorio, K. Riska and P. Varsta (1979).
29. ON THE DRIFT AND DEFORMATION OF SEA ICE FIELDS IN THE BOTHNIAN BAY. M. Leppäranta (1980).
30. A SENSITIVITY OF STEADY FREE FLOATING ICE. A. Omstedt (1980).
31. A STUDY OF THE LARGE SCALE COOLING IN THE BAY OF BOTHNIA. J. Sahlberg and H. Törnevik (1980).
32. STATISTICAL FEATURES OF SEA ICE RIDGING IN THE GULF OF BOTHNIA. M. Leppäranta (1980).
33. PERFORMANCE OF MARINE PROPELLERS IN ICE-CLOGGED CHANNELS. V. Kostilainen (1980).
34. BASIS - A data bank for Baltic sea ice and sea surface temperatures. I. Udin, S. Uusitalo, J. Sahlberg, A. Seinä, J-E. Lundqvist and M. Leppäranta (1981).



